https://doi.org/10.5194/egusphere-2026-6649
Preprint. Discussion started: 13 November 2026
© Author(s) 2026. CC BY 4.0 License.

Common Era Hydroclimate in south-eastern Australia: a decadal-scale diatom-inferred salinity record from Lake Bullen Merri, Victoria

Mahfuzur Rahman [1,2*], Kym Edwards [1], Özlem Karadaş [3], Wojciech Tylmann [4], Bernd Zolitschka [3], Keely Mills [5], Victoria Miller [6], Haidee Cadd [7], Martin Ankor [1], Cameron Barr [1], Alexander Francke [1], David Child [8], Geraldine Jacobsen [8], Michael Hotchkis [8], John Tibby [9], Jonathan Tyler [1]

[1] School of Physics, Chemistry and Earth Science, Adelaide University, Australia
[2] Department of Oceanography, Noakhali Science and Technology University, Noakhali, Bangladesh
[3] Institute of Geography, University of Bremen, Germany
[4] Department of Geomorphology and Quaternary Geology, University of Gdansk, Poland
[5] British Geological Survey, United Kingdom
[6] School of Culture History & Language, Australian National University, Australia
[7] Environmental Futures, University of Wollongong, Australia
[8] Centre for Accelerator Science, Australian Nuclear Science and Technology Organisation (ANSTO), NSW, Australia
[9] Geography, Environment and Population, Adelaide University, Australia

Correspondence: Mahfuzur Rahman

Email: mahfuzur.rahman@adelaide.edu.au & mahfuz916@gmail.com

https://doi.org/10.5194/egusphere-2026-6649
Preprint. Discussion started: 13 November 2026
© Author(s) 2026. CC BY 4.0 License.



Abstract

Understanding past hydroclimate variability at decadal scales over multiple centuries is critical for assessing the potential recurrence of prolonged droughts and floods and for informing sustainable environmental and economic planning. This study presents a sub-decadal to decadal hydroclimate reconstruction spanning the last ~2500 years from Lake Bullen Merri, a ~58 m deep maar lake in south-eastern Australia. Lake water salinity, recorded as electrical conductivity (EC), is inferred from sedimentary diatom assemblages. A chronology is established using nine AMS radiocarbon (^{14}C) dates on pollen concentrates, ^{210}Pb dating, plutonium concentrations, and the first appearance of exotic *Pinus* pollen. EC, which is inversely related to lake water volume, reveals a prolonged high lake-level phase between ~1380 and 1750 CE, which overlaps with the Little Ice Age (LIA). Prior to this, lake water EC was higher, characterised by three prominent centennial-scale periods of high EC and lower lake levels leading up to the last quarter of the first millennium of the common era (CE). Using a new calibration model for diatom-inferred EC reconstructions, we compare our record to diatom records from nearby Tower Hill Main Lake, Lake Elingamite and Lake Surprise which show broadly similar patterns, indicating a coherent hydroclimate signal in the western Victorian maar lakes. Overall, these records confirm that the LIA was a comparatively wet interval in south-eastern Australia, followed by drying in the late eighteenth and nineteenth centuries. This contrast is not clearly expressed in existing tree-ring and ice-core-derived reconstructions, most of which began during the wet phase. Together, these records show that south-eastern Australian hydroclimate shifted between wetter and drier states on multi-decadal to multi-centennial timescales. This much broader range of hydroclimatic variability compared to those represented by shorter reconstructions provides the needed baseline for long-term water-resource planning.

Keywords: Hydroclimate variability; Lake levels; Diatoms; Electrical conductivity; Transfer function; Maar lakes; Little Ice Age.

https://doi.org/10.5194/egusphere-2026-6649
Preprint. Discussion started: 13 November 2026
© Author(s) 2026. CC BY 4.0 License.

1 Introduction

Decadal-scale hydroclimate extremes, such as prolonged droughts and periods of higher precipitation, have major impacts on Australia's people, ecosystems, and economy, yet their long-term patterns are still not well understood (Chamberlayne et al., 2023; Kiem et al., 2016; Palmer et al., 2024; Rahman et al., 2025). The last 2000 years are particularly important because this period provides essential context for recent human-driven climate change and a baseline for Earth's natural climate variability (Emile-Geay et al., 2017). By improving records of hydroclimate variability over the past two millennia, especially on decadal to centennial timescales, we can better validate climate models, assess climate sensitivity to external forcing, and evaluate the likelihood of prolonged extreme events (Armstrong et al., 2020; Barr et al., 2014; Cook et al., 2016; Falster et al., 2024; Kiem et al., 2016; Steiger et al., 2018). This is particularly important as instrumental climate records in Australia only extend to the start of the 19th century at most and therefore do not capture the full continuum of hydroclimate variability.

Annually resolved tree-ring and coral records provide valuable hydroclimate archives, capturing decadal-scale extremes such as droughts and floods, and supporting reconstructions of past river discharge (e.g. Cook et al., 2022; Freund et al., 2017; O'Donnell et al., 2021; Palmer et al., 2024). However, in Australia, tree-ring and coral based hydroclimate reconstructions rarely extend beyond 1200 CE with most beginning between approximately 1400 and 1600 CE (Freund et al., 2017). In addition, tree-ring reconstructions can be subject to methodological limitations, including the potential attenuation of low-frequency variability during standardisation (Cook et al., 1995), temporal instability in climate–growth relationships (D'Arrigo et al., 2008), sensitivity to statistical and modelling choices (Schofield et al., 2016), and challenges in scaling site-level tree-growth signals to regional hydroclimate estimates (Babst et al., 2018). Some studies have used archives from climatically distal regions, including Antarctic ice cores and Chinese speleothems, to infer hydroclimate variability in parts of southern Australia (Goodwin et al., 2014; McGowan et al., 2009; Van Ommen and Morgan, 2010; Tozer et al., 2016; Vance et al., 2013, 2015). However, significant uncertainties remain about whether the modern day climate teleconnections are stable beyond their calibration period and geographic scope (Dätwyler et al., 2018; Gallant et al., 2013). In this context, lake sediments offer a valuable source of data, being located within the regions of interest. Lakes and lake sediments offer direct insights into hydrological variability with the potential to reconstruct past hydroclimate at sub-decadal timescales over multiple millennia using a wide range of proxies (Barr et al., 2014; Bird et al., 2011; Holmes et al., 2023; Sepúlveda-Zúñiga et al., 2022; Viana et al., 2014). However, while several lake- or wetland-based hydroclimate reconstructions exist for south-eastern Australia (e.g. Gouramanis et al., 2010; Kemp et al., 2012; Wilkins et al., 2013; Zheng et al. 2025) relatively few records have the sub-decadal temporal resolution which is required to resolve hydroclimate variability on a timescale relevant to contemporary environmental challenges (Barr et al., 2014; Chamberlayne et al., 2023; Rahman et al.,

https://doi.org/10.5194/egusphere-2026-6649
Preprint. Discussion started: 13 November 2026
© Author(s) 2026. CC BY 4.0 License.

2025; Saunders et al., 2012). Consequently, there is a continued need for new high-resolution lake sediment records with robust and quantifiable links to hydroclimate.

Lakes are sensitive recorders of environmental change, and their sediments can preserve detailed histories of climate and hydrological variability over a wide range of timescales. Although human activities in lake catchments complicate any interpretation, lake ecosystems typically respond strongly to climate variability, and these responses are archived in the accumulating sediments (Battarbee, 2000). Crater and maar lakes are especially valuable in this regard because their small, enclosed catchments and restricted inflows and outflows make them highly responsive to changes in regional climate, particularly effective moisture, here defined as the balance between precipitation and evaporation that controls water availability in the catchment (Wang et al., 2012; Zolitschka et al., 2000). Among the biological remains preserved in lake sediments, diatoms are particularly useful indicators of environmental conditions and have been widely used to reconstruct Holocene climate variability (Barr et al., 2014; Gell, 1998; Sepúlveda-Zúñiga et al., 2022; Viana et al., 2014; Zou et al., 2021).

Diatoms are highly sensitive to environmental change in aquatic systems, and many taxa have narrow ecological tolerances for water chemistry variables such as salinity (Fritz et al., 1991; Gell, 1997; Reid et al., 1995). Their widespread occurrence, high abundance, rapid reproduction, and well-developed taxonomy make them particularly effective as bioindicators (Battarbee et al., 2001; Smol and Douglas, 2007). In closed-basin lakes of arid and semi-arid regions, changes in effective moisture strongly influence salinity through the concentration or dilution of dissolved salts, and these changes are clearly reflected in shifts in diatom assemblages (Fritz et al., 1991). Australian studies have shown strong statistical relationships between diatom distributions and lake-water salinity (Blinn, 1995; Gell, 1997; Gell and Gasse, 1994; Tibby et al., 2007). These relationships allow past salinity to be quantitatively reconstructed from diatom assemblages, providing insight into hydroclimatic variability over timescales ranging from decades to millennia. To reconstruct past salinity, transfer functions based on modern calibration datasets are widely used for this purpose because they relate diatom species to their preferred salinity optima. These functions can then be applied to fossil diatom assemblages from sediment cores to infer past salinity changes and, by extension, hydroclimate variability in the lake's catchment (Laird et al., 2011; Yang et al., 2003). Weighted averaging (WA) and weighted-averaging partial least squares (WA-PLS) regression are widely used to develop transfer functions because they are statistically robust and easy to implement (Birks, 2012).

Relatively few diatom-based salinity or EC transfer functions have been developed for inland waters in Australia (e.g. Barr, 2010; Gell, 1997; Taukulis and John, 2009), and these are typically restricted to limited geographic regions. This narrow spatial coverage limits the ecological interpretation of diatom taxa and reduces the robustness of inferred environmental optima (Juggins, 2013). For transfer functions to be effective, their training sets must include modern sites that are good analogues for potential past

https://doi.org/10.5194/egusphere-2026-6649
Preprint. Discussion started: 13 November 2026
© Author(s) 2026. CC BY 4.0 License.

conditions. For example, a previous reconstruction of past EC from two western Victorian lakes was hampered by numerous no-analogue samples, indicating that the calibration dataset did not fully capture the environmental conditions reflected in the fossil assemblages (Barr et al., 2014). Rahman et al. (2026) addressed this limitation by developing a diatom–EC transfer function based on 475 samples from 226 lakes across a broad environmental gradient. The resulting species-specific EC optima provide a robust basis for inferring past hydroclimatic variability from lake sediment diatom records in south-eastern Australia.

Tyler et al. (2015) demonstrated that four nearby, decadal resolved diatom records from western Victoria had coherent regional-scale environmental patterns over the last millennium, highlighting the value of multi-record approaches for distinguishing broader hydroclimate signals from site-specific variability. Likewise, Tibby et al. (2018) inferred that eastern Australia was relatively wetter during the Little Ice Age (1500–1850 CE) with the region experiencing subsequent drying, emphasizing the importance of placing late-Holocene hydroclimate change in a longer historical context. These studies contrast with tree ring and ice core-based reconstructions, which imply relatively weak centennial-scale hydroclimate variability over the last millennium in Australia (Higgins et al., 2023; O'Donnell et al., 2021; Palmer et al., 2024; Vance et al., 2015). The current study aims to address this disparity by developing a new diatom-inferred hydroclimate record with sub-decadal to decadal resolution from Lake Bullen Merri, Victoria, along with re-calibration of three previously published diatom records from the same region. We use a new diatomf–EC transfer function (Rahman et al., 2026) to infer past changes in lake-water conductivity and interpret these changes as variations in effective moisture and hydroclimate extremes. Our primary aim is to reconstruct past hydroclimate variability and assess whether the signal is coherent across the four records. This comparison also allows us to test the hypothesis of a wet Little Ice Age in south-eastern Australia, relative to the hydroclimatic state during centuries before and afterwards. Together, these records provide a high-resolution, multi-site view of late-Holocene hydroclimate in south-eastern Australia.

2 Materials and methods

2.1 Study Area

Lake Bullen Merri is a cloverleaf-shaped volcanic crater lake (Jones et al., 2001) located near Camperdown, Victoria, Australia (38.248725 °S, 143.103935 °E) **(Fig. 1a & b)**. The region experiences a temperate climate, with a mean annual temperature of ~13 °C, ranging from 18.0 °C in summer to 8.2 °C in winter. Average annual rainfall is ~775 mm, mainly between May and November, while annual evaporation is ~1250 mm based on daily data from the Australian Bureau of Meteorology from 1970 to 2017, interpolated and made accessible via the SILO database (Ankor, 2020; Jeffrey et al., 2001). The lake has a current maximum depth of approximately 60 m (139.5 m Australian Height Datum (AHD), September 2018), a surface area of about 4.35 km², and a catchment area of approximately 8.86 km²

https://doi.org/10.5194/egusphere-2026-6649
Preprint. Discussion started: 13 November 2026
© Author(s) 2026. CC BY 4.0 License.

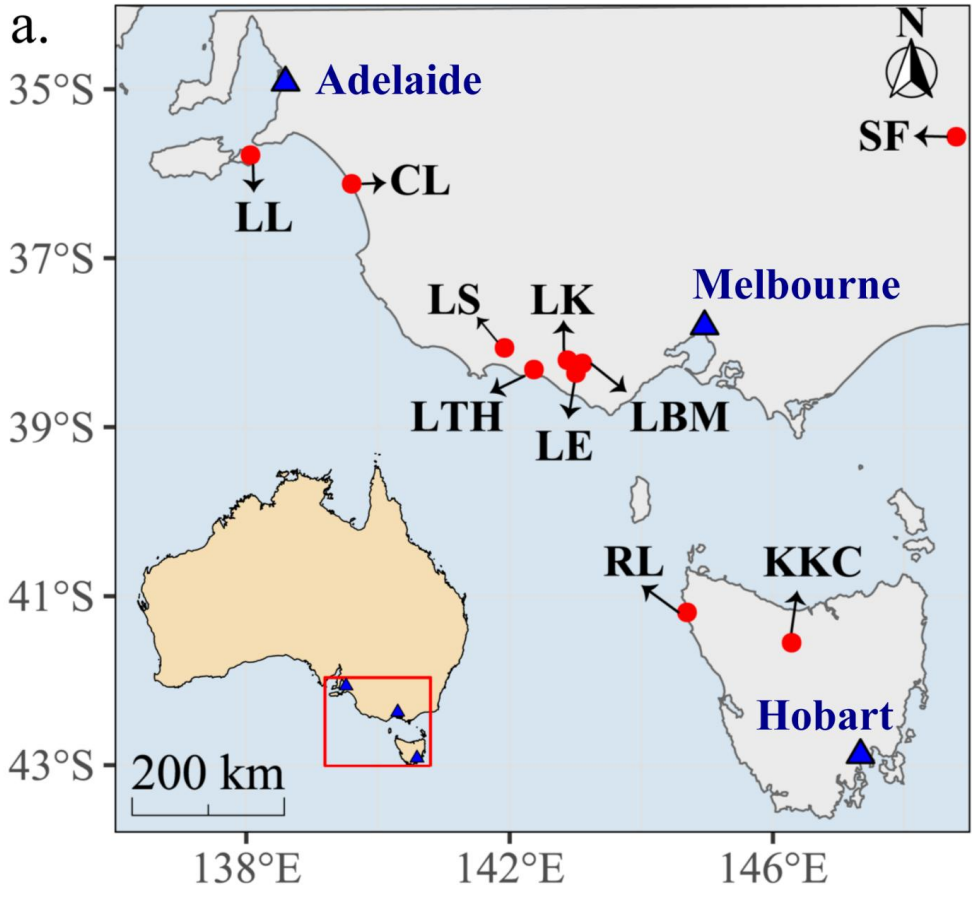
(Ankor, 2020). It was formed through multiple eruptive events and has steep cone-shaped slopes with a relatively flat centre (Jones et al., 2001). The entire catchment lies within the crater, with no surface inflow or outflow and minimal input from groundwater. As a result, lake levels are primarily controlled by the balance between precipitation and evaporation (Jones et al., 2001; Leahy, 2010). Historically, Lake Bullen Merri was full at around 1841 CE, reaching approximately 168.4 m AHD (Ankor, 2020) and was overflowing into Lake Gnotuk (Currey, 1970). After 1841 CE, the lake level declined (Tibby and Tiller, 2007).

Since the 1970s, Lake Bullen Merri has been the focus of multiple limnological and paleoenvironmental investigations. Regional limnological surveys have shown that Lake Bullen Merri is a moderately saline, sodium–chloride-dominated, alkaline crater lake exhibiting minor seasonal salinity changes (De Deckker and Williams, 1988). Lake Bullen Merri also exhibited relatively stable electrical conductivity values between autumn 1992 and autumn 1997 (mean: 13,997 µS/cm; SD: 962 µS/cm) (Tibby and Tiller, 2007). During fieldwork on 23 November 2023, water samples were collected at depths ranging from 0.5 m to 52 m and analysed for physicochemical parameters (cf., supplementary data). Along the depth profile, the lake water is consistently alkaline, with pH values ranging from 8.73 to 8.89 (average: 8.81). Electrical conductivity ranges from 16,800 to 17,600 µS/cm (average: ~17,183 µS/cm), and total dissolved solids range from 10,900 to 11,400 mg/L (average: ~11,158 mg/L), indicating highly saline conditions. Total alkalinity varies between 767 and 789 mg/L (average: ~776 mg/L as $CaCO_3$). Chloride concentrations are very high, ranging from 5,490 to 5,680 mg/L (average: ~5,558 mg/L), while sulphate remains very low at 2–3 mg/L. Major cations are dominated by sodium (2,960–3,080 mg/L; average: ~3,000 mg/L), followed by magnesium (295–308 mg/L; average: ~299 mg/L), with relatively low values of calcium (13–14 mg/L) and potassium (118–123 mg/L). Reactive silica concentrations range from 0.8 to 0.9 mg/L. Nutrient concentrations are moderate to high, with ammonia ranging from <0.01 to 1.24 mg/L, nitrite from <0.01 to 0.44 mg/L, nitrate (as N) from <0.01 to 0.31 mg/L, reactive phosphorus from <0.01 to 0.10 mg/L, and nitrite + nitrate (as N) ranging from <0.01 to 0.47 mg/L; however, slight increases in nitrogen species are observed with depth. Previous hydrologic and isotopic modelling has demonstrated that Lake Bullen Merri's water balance is dominated by precipitation–evaporation, with only minor groundwater exchange, and that combined lake-level and isotope data can be used to reconstruct past effective moisture and regional climate (Ankor, 2020; Jones et al., 2001). Lake level (m AHD) and lake-water electrical conductivity exhibit a pronounced inverse relationship from 1889–2018 CE, underscoring the strong control of lake volume on salinity in this closed-basin maar system (Ankor, 2020).

Late Pleistocene pollen analysis from deep central cores at Lake Bullen Merri documents regional vegetation change and lake-level fluctuations over the last ~16,000 years (Dodson, 1979). Fossil diatom and ostracod studies from Lake Bullen Merri and nearby maar lakes were interpreted to reflect synchronous Holocene changes in water level and salinity, including high stands between ~4,450 and

https://doi.org/10.5194/egusphere-2026-6649
Preprint. Discussion started: 13 November 2026
© Author(s) 2026. CC BY 4.0 License.

1,850 BCE and significant declines over the last century (De Deckker, 1982). Duthie (2000) analysed diatoms in a sediment core from Lake Bullen Merri and applied transfer functions to infer salinity over the last ~4,500 years. The record indicates an early phase (about 2,550–1,850 BCE) with relatively high salinity followed by a long interval (about 1,850–150 BCE) in which *Nitzschia frustulum* reached 100% abundance, implying much lower salinity. Between roughly 50 BCE and 1,450 CE, diatom assemblages point to periods of lower salinity, after which salinity is inferred to have risen markedly during the last ~500 years, consistent with historical lake-level decline and post-European settlement. This previous study of the diatoms of Lake Bullen Merri highlights the potential to develop a hydroclimate reconstruction, subject to improved chronology, higher temporal resolution and statistically sound calibration.



https://doi.org/10.5194/egusphere-2026-6649
Preprint. Discussion started: 13 November 2026
© Author(s) 2026. CC BY 4.0 License.

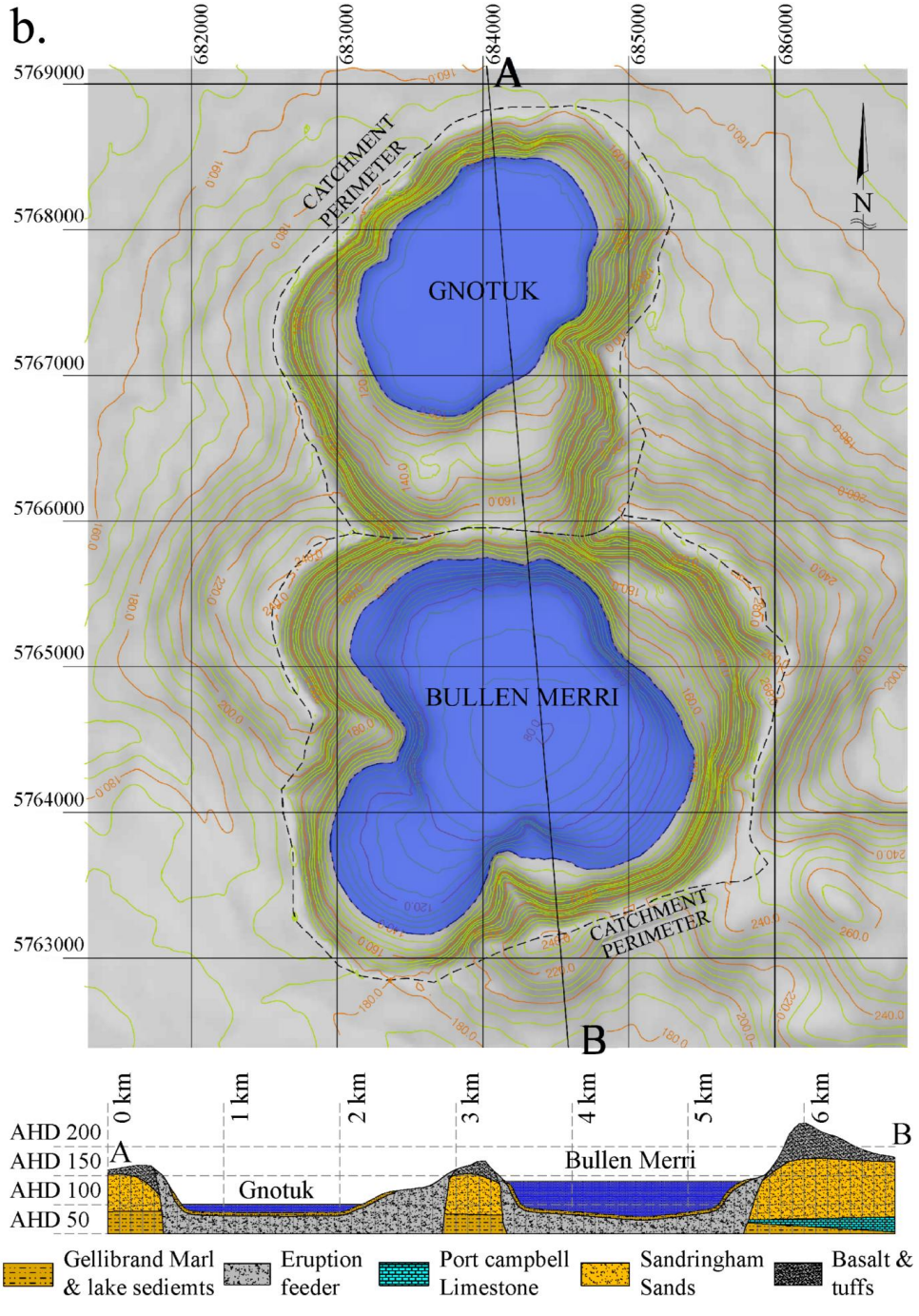


Figure 1. Location map of the study area. (a.) Regional map showing the primary study site, Lake Bullen Merri (LBM), and nearby maar lakes Lake Elingamite (LE), Lake Surprise (LS), Lake Tower

https://doi.org/10.5194/egusphere-2026-6649
Preprint. Discussion started: 13 November 2026
© Author(s) 2026. CC BY 4.0 License.

Hill (LTH), and Lake Keilambete (LK), together with more distant comparison sites Coorong Lagoon (CL), Lashmars Lagoon (LL), Snowy Flat (SF), Rebecca Lagoon (RL), and Kubla Khan Cave (KKC); the red box indicates their overall location within Australia. (b.) Detailed view of the Lake Bullen Merri catchment, showing topography, current water level, and geological formations in cross-section along transect A–B. Panel (b) is modified from Ankor (2020).

2.2 Core recovery and sediment sampling

A total of seven sediment cores were collected from Lake Bullen Merri at water depths between 58–60 m on 23 November 2023. Four ~1 m long cores (BUL23-1, BUL23-2, BUL23-3, BUL23-4) were obtained using a UWITEC gravity corer, and three ~2.5 m long cores (BUL23-5, BUL23-6, BUL23-7) were collected using a hammer-driven piston corer (Chambers and Cameron, 2001). Each of the three piston cores was cut into three sections, which were labelled by appending a decimal suffix to the core ID (e.g. BUL23-5.1, BUL23-5.2 and BUL23-5.3 for the three sections of core BUL23-5). All core sections were split longitudinally and visually described (colour, grain size, sedimentary structures, consistency, and macrofossil content) at the GEOPOLAR Laboratory, University of Bremen, Germany. High-resolution elemental analyses were subsequently carried out with an ITRAX X-ray fluorescence (XRF) core scanner at the same laboratory. Following this, core BUL23-3 and sections BUL23-5.1, 5.2 and 5.3 were sampled at 0.5 cm intervals, and each slice was sealed in a plastic polypropylene bag and labelled with a unique code. During sectioning, some millimetres of sediment were lost, creating gaps in otherwise continuous sequences; to address this, overlapping cores were correlated to construct a composite depth profile.

Core-to-core correlation was performed using the centred log-ratio–transformed titanium record (Ti-clr), chosen because Ti is relatively immobile, and predominantly hosted in detrital minerals, making it a robust, redox-insensitive proxy for terrigenous input (Gebregiorgis et al., 2020; Gong et al., 2020; Thöle et al., 2020). Although we evaluated other elements measured by XRF core scanning (Si, K, Ca, Mn, Fe, Sr), Ti-clr showed the clearest and most laterally consistent peaks and troughs across all core sections providing the best and unambiguous features for core correlation. The clr transformation was applied to account for the compositional (closed-sum) nature of the XRF intensity data (Kerfriden et al., 2025; Mondal et al., 2021; Weltje and Tjallingii, 2008).

2.3 Chronology

Age–depth models were constructed by combining radiocarbon dating from older sediment sections **(Table 1)** with ^{210}Pb activity profiles **(Fig. 2a)**, Pu concentration and isotope ratios **(Fig. 2b)**, and stratigraphic markers such as the first occurrence of exotic *Pinus radiata* pollen from the upper core section. An age–depth model was developed for the composite record using the rPlum package in R (Aquino-López et al., 2018; Blaauw and Christen, 2011). Radiocarbon samples and Pu samples were processed and analysed at the Centre for Accelerator Science, Australian Nuclear Science and

https://doi.org/10.5194/egusphere-2026-6649
Preprint. Discussion started: 13 November 2026
© Author(s) 2026. CC BY 4.0 License.

Technology Organisation (ANSTO). AMS ^{14}C dates were conducted on pollen concentrates following Cadd et al., (2022), while Pu analysis followed the methods of Child et al. (2008) and Hotchkis et al. (2019). Radiocarbon ages were calibrated using the SHCal20 calibration curve (Hogg et al., 2020) and are reported in calibrated years before present (BP, where "present" = 1950 CE). The activity concentrations of total ^{210}Pb were determined indirectly by measuring its daughter product ^{210}Po (α = 5.308 MeV, $T_{1/2}$=138 d) using alpha spectrometry at the Paleoenvironmental Research Laboratory, University of Gdańsk, Poland (Tylmann et al., 2016).

Exotic pine (*Pinus radiata)* pollen, introduced to Australia following European colonisation, provides a useful chronostratigraphic marker of post-colonial European settlement and agricultural expansion (Tibby et al., 2003). In Victoria, *P. radiata* seedlings were first raised at the Macedon nursery in 1872 and planted specifically for forestry at Macedon in 1880; planting was subsequently expanded from 1888 onwards (Australian Academy of Technological Sciences and Engineering, 1988; Victoria's Forestry & Bushfire Heritage, 2022). Under favourable conditions, *P. radiata* typically begins producing cones and substantial quantities of pollen approximately 5–10 years after planting, implying a relatively short time lag between plantation establishment and likely deposition of pollen in nearby sediments. Twenty-one sediment samples from 1.1–100.4 cm of the composite depth sequence were prepared for pollen analysis. Pollen samples were processed from 0.5 cc of sediment using the protocol outlined in Duxbury et al. (2026) and slides from 1.1 – 54.8 cm were scanned for *Pine* pollen.

2.4 Diatom analysis

Sediment cores were stored at 4°C in the dark until processing. Cores were sliced into 0.5-cm sections, but diatom samples were analysed at approximately 1 cm depth intervals by preparing slides from every second 0.5 cm section. Diatom samples were processed using HCl and H_2O_2 following the digestion methods described by Battarbee et al. (2001) and Renberg (1990) to remove carbonates and organic matter, respectively. After digestion and rinsing, the final suspensions were gently agitated, and 200 µL aliquots were pipetted onto microscope coverslips that already contained 300 µL of distilled water to promote an even spread of frustules. Coverslips were allowed to dry, then inverted and mounted on microscope slides using Naphrax (refractive index = 1.73). Diatom identification and counting were carried out at 1000× magnification using a Zeiss Axio Scope A1 transmission microscope equipped with an oil-immersion objective. For each sample, a minimum of 300 diatom valves was counted and used to calculate the percentage abundance of each taxon. Species were identified with reference to (Krammer and Lange-Bertalot, 1986, 1988, 1991b, a), using their dichotomous keys and illustrations, and cross-checked against the Diatom Flora of Australia (John, 2016, 2018, 2020) and Diatoms of North America (Spaulding and al., 2021) for regional taxa.

https://doi.org/10.5194/egusphere-2026-6649
Preprint. Discussion started: 13 November 2026
© Author(s) 2026. CC BY 4.0 License.

2.5 Statistical methods

Diatom assemblages were divided into stratigraphic zones using stratigraphically CONstrained Incremental Sum of Squares (CONISS) cluster analysis (Grimm, 1987). This method groups samples based on their compositional similarity while preserving their stratigraphic order, allowing identification of major ecological shifts through time. To ensure that the identified zones were statistically meaningful, the results of the CONISS analysis were evaluated using the broken-stick model (Bennett, 1996). This approach compares the observed dispersion at each cluster split with that expected under a random (null) distribution. Only those splits where the observed variance exceeded the broken-stick expectation were accepted as significant. Both manual inspection and automated comparison were used to assess these splits. This step reduces the risk of over-interpreting minor fluctuations and ensures that only robust, non-random assemblage changes define zonation.

Past lake water conductivity was reconstructed using a diatom-based electrical conductivity (EC) transfer function developed by Rahman et al. (2026). This training set is the largest of its kind to date, based on 475 samples from 226 lakes and comprising 578 diatom taxa across a broad salinity gradient (25–195,800 µS/cm). The model was developed using weighted averaging with inverse deshrinking and shows strong predictive performance, with a cross-validated coefficient of determination ($r^2_{jackknifed}$ = 0.843) and a low root mean squared error of prediction (RMSEP = 0.38 $\log_{10}$ µS/cm) (Rahman et al., 2026). This transfer function was applied to the fossil diatom record from Lake Bullen Merri to infer past conductivity changes. Fossil and modern diatom assemblages were taxonomically harmonised prior to reconstruction. Taxa absent from the modern calibration dataset were excluded from transfer-function calculations. Taxonomic representation was quantified for each fossil sample as the cumulative relative abundance of taxa represented in the modern calibration dataset. Reconstructions were compared across several methods, including weighted averaging (WA), weighted averaging with inverse deshrinking (WA-Inv), weighted averaging with classical deshrinking (WA-Cla), locally weighted averaging with inverse deshrinking (LWWA-Inv), locally weighted averaging with classical deshrinking (LWWA-Cla) and weighted averaging partial least squares (WA-PLS), to assess consistency and robustness. All statistical analyses were conducted using the software C2 version 1.8 (Juggins, 2022), along with the R packages rioja (Juggins, 2024) and vegan (Oksanen et al., 2025).

In addition to Lake Bullen Merri, three previously published fossil diatom records from nearby sites were re-calibrated using the Rahman et al. (2026) transfer function to enable regional comparison of conductivity changes. Two of these records, from Lake Elingamite and Lake Surprise, were originally published in Barr et al. (2014), and the third, from Tower Hill Main Lake, was published in Mills et al. (2013) and later used by Tyler et al. (2015) but is presented here for the first time as an EC reconstruction. Applying a consistent transfer function across all records allows for a more robust comparison of regional hydroclimatic variability. The chronology for the Lake Surprise diatom record

https://doi.org/10.5194/egusphere-2026-6649
Preprint. Discussion started: 13 November 2026
© Author(s) 2026. CC BY 4.0 License.

was updated from Barr et al. (2014) to that published by Dharmarathna et al. (2025) on the basis of correlating XRF-inferred Ca from core SUR19-1 (Dharmarathna et al., 2025) to loss on ignition-based estimates of carbonate concentration from core LS01 (Barr et al., 2014).

3 Results

3.1 Core correlation

Ti-clr was plotted against core depth for all sections, with similar sections arranged adjacent to aid comparison, and corresponding peaks and troughs were matched between cores to define 30 stratigraphic tie points **(Fig. S1).** Composite depths were assigned to each tie point relative to a designated reference core, and core depths were converted to composite depth by linear interpolation between the tie points in R. As some tie points are very close to the top and bottom of each core, interpolation essentially constrained the entire length of every core, leaving only negligible terminal extrapolation, so the resulting composite depth profile is well anchored throughout.

Correlation was validated by replotting both Ti-clr and the independent Ca-clr records against the composite depth scale **(Fig. S2)**. Both aligned excellently across all cores; because Ca-clr was not used to define the tie points, its agreement provides an independent internal check confirming the robustness of the Ti-based composite depth model. Despite the robust composite-depth model, diatom samples are unavailable for the 152.1–163.2 cm composite-depth interval. Although the missing interval in cores BUL23-5.1 and BUL23-5.2 was represented by overlapping material from core BUL23-7.2 and incorporated into the composite-depth model, the relevant BUL23-7.2 section remained at the GEOPOLAR Laboratory in Bremen and could not be transported to Adelaide for diatom analysis in the available timeframe. Consequently, the diatom record contains a data gap across this interval, and no diatom-inferred electrical-conductivity values were interpolated across the gap.

3.2 Chronology

The ^{210}Pb data show unsupported activities that decrease with depth **(Fig. 2a)**, as expected for a constantly accumulating sedimentary sequence. These data are supported by total Pu concentration data, which reached a maximum value of 0.602 ± 0.0135 (pg/g) at 18.9 cm, before decreasing towards the uppermost sediments. This maximum was interpreted as the Southern Hemisphere peak in fallout from atmospheric nuclear-weapons testing and was assigned an age of 1964 CE (Hancock et al., 2011; Walling and Meyers, 2012). The measured ^{240}Pu/ ^{239}Pu isotopic ratios **(Fig. 2b)** have a weighted mean value of 0.162 ± 0.002, in reasonable agreement with the mean ratio of 0.172 ± 0.007 reported for Bathurst Harbour, Tasmania (Harrison et al., 2021) and the mean ratio of 0.142 ± 0.004 reported for Lake Surprise, Victoria (Dharmarathna et al., 2025).

P. radiata pollen was identified for pollen samples from 1.1 – 39.2 cm. The first *Pinus* pollen appears at 39.9 cm composite depth and displays a gradual increase in abundance from 39.9 cm to the top of the

https://doi.org/10.5194/egusphere-2026-6649
Preprint. Discussion started: 13 November 2026
© Author(s) 2026. CC BY 4.0 License.

sediment profile. The first appearance of *Pinus* pollen is interpreted to date to approximately 1890 CE, consistent with documented early regional establishment of *P. radiata* pine and landscape-scale pollen dispersal (Lavery and Mead, 1998). This interpretation deliberately draws on historical and biological information because the ^{210}Pb profile from 0–34.5 cm did not capture the time frame of *Pinus* appearance. The lowest detectable ^{210}Pb horizon occurred at 27.4 cm sediment depth and had a mean modelled age of approximately 1913 CE based on the Plum age-depth model. Consequently, the *Pinus* pollen first detected at 39.9 m lies beyond the effective dating range of the ^{210}Pb method, necessitating the use of literature-based constraints on *P. radiata* introduction and maturation to anchor this horizon at ~1890 CE.

An age depth model for the record was developed using a combination of AMS ^{14}C dates, ^{210}Pb, Pu isotopes, the first detection of *Pinus* pollen and the coring date of November 2023. Three AMS ^{14}C measurements that yielded uncalibrated ages inconsistent with the ^{210}Pb data, and the *P. radiata* pollen horizon were treated as outliers and excluded a priori from the Bayesian age–depth modelling, while nine AMS ^{14}C ages were used in the development of the Bayesian age-depth model. This approach prioritises the most robust independent age markers, and sensitivity tests showed that including the outlying ^{14}C ages had only a negligible influence on the resulting age–depth model **(Table 1)**. Ages reported for each depth are the weighted means of their posterior age distributions, with uncertainties derived from Monte Carlo simulations, yielding a coherent probabilistic chronology.

Table 1. Radiocarbon (^{14}C) dating results for Lake Bullen Merri pollen extract samples, including conventional ^{14}C ages (yr BP) and modelled sediment ages (yr BP).

ANSTO Code	Composite depth (cm)	δ^{13}C (‰) ± 1σ	pMC ± 1σ	Conventional ^{14}C age (yr BP) ± 1σ	Modelled age (yr BP); mean (min–max)
OZBZ12	19.4	-25*	85.96 ± 0.87	1220 ± 90	NA
OZBZ13	44.6	-25*	91.09 ± 1.12	750 ± 100	NA
OZBZ15	54.8	-7.9 ± 0.4	91.91 ± 0.96	680 ± 85	NA
OZBZ25	64.1	−9.1 ± 1.9	94.28 ± 0.26	470 ± 25	420 (330–500)
OZBZ14	74.3	−15.4 ± 0.5	93.38 ± 0.28	550 ± 25	530 (500–610)
OZBZ16	104.5	−16.1 ± 0.8	87.12 ± 0.9	1110 ± 90	860 (760–960)
OZBZ11	106.5	−17.2 ± 0.4	88.24 ± 0.67	1000 ± 70	890 (780–980)
OZBZ26	113.1	−25 *	85.77 ± 0.67	1230 ± 70	960 (820–1060)
OZBZ17	139.3	−19.3 ± 0.3	89.22 ± 0.73	920 ± 70	1160 (1010–1280)
OZBZ18	168.8	−25.7 ± 0.3	83.52 ± 0.73	1450 ± 70	1440 (1290–1620)

https://doi.org/10.5194/egusphere-2026-6649
Preprint. Discussion started: 13 November 2026
© Author(s) 2026. CC BY 4.0 License.

OZBZ19	223.5	−25 *	75.56 ± 0.71	2250 ± 80	2180 (1950–2370)
OZBZ37	283.7	−25 *	64.42 ± 0.61	3530 ± 80	2960 (2530–3450

* assumed value – unable to be measured due to small mass; NA = not applicable; modelled ages are not reported for samples whose radiocarbon dates were excluded from the age–depth model.

The Bayesian rPlum model estimates that the deepest analysed sample (composite depth 283.7 cm) has a mean age of 2,960 cal yr BP (1010 BCE) **(Fig. 3)**. This age–depth model provides the chronological framework for the diatom-based environmental reconstructions presented below. A Bayesian age–depth model for the Tower Hill Main Lake diatom record was developed from four previously obtained AMS ^{14}C ages (Mills et al. 2013; Tyler et al. 2015) and the first appearance of *Pinus* pollen. The resulting age–depth model is presented in the supplementary material **(Fig. S3)**. The four radiocarbon ages form a stratigraphically coherent set, with ages increasing with depth within their calibrated uncertainties. For Lake Elingamite, the age–depth model follows Barr et al. (2014), with recalibrated ^{14}C ages, whereas the Lake Surprise diatom record uses the updated chronology published by Dharmarathna et al. (2025).

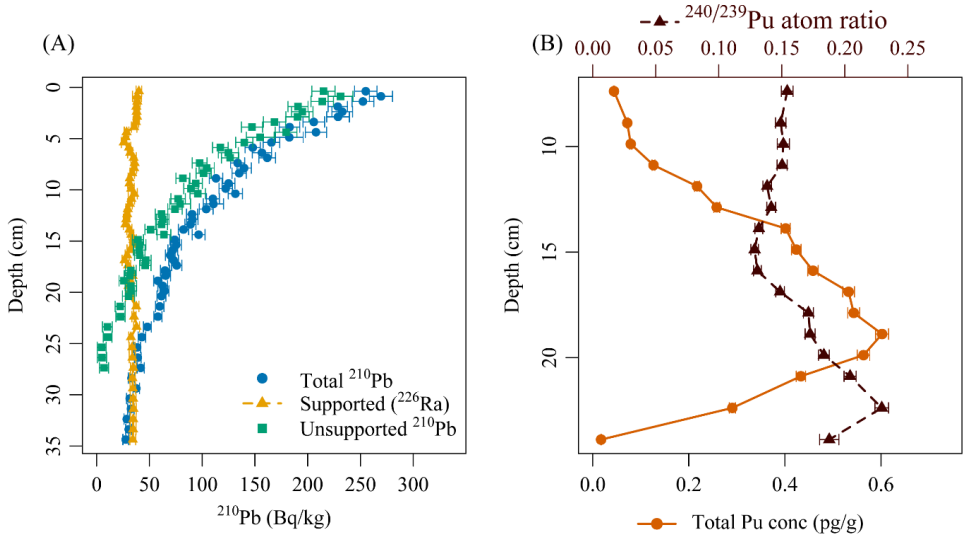


Figure 2. (A) Total, supported and unsupported ^{210}Pb activities plotted against depth, illustrating the decay of unsupported ^{210}Pb with depth and its distinction from supported activity. Panel (B) marks the position of the Pu-isotope peak corresponding to 1964 CE, used as an independent chronological anchor.

https://doi.org/10.5194/egusphere-2026-6649
Preprint. Discussion started: 13 November 2026
© Author(s) 2026. CC BY 4.0 License.

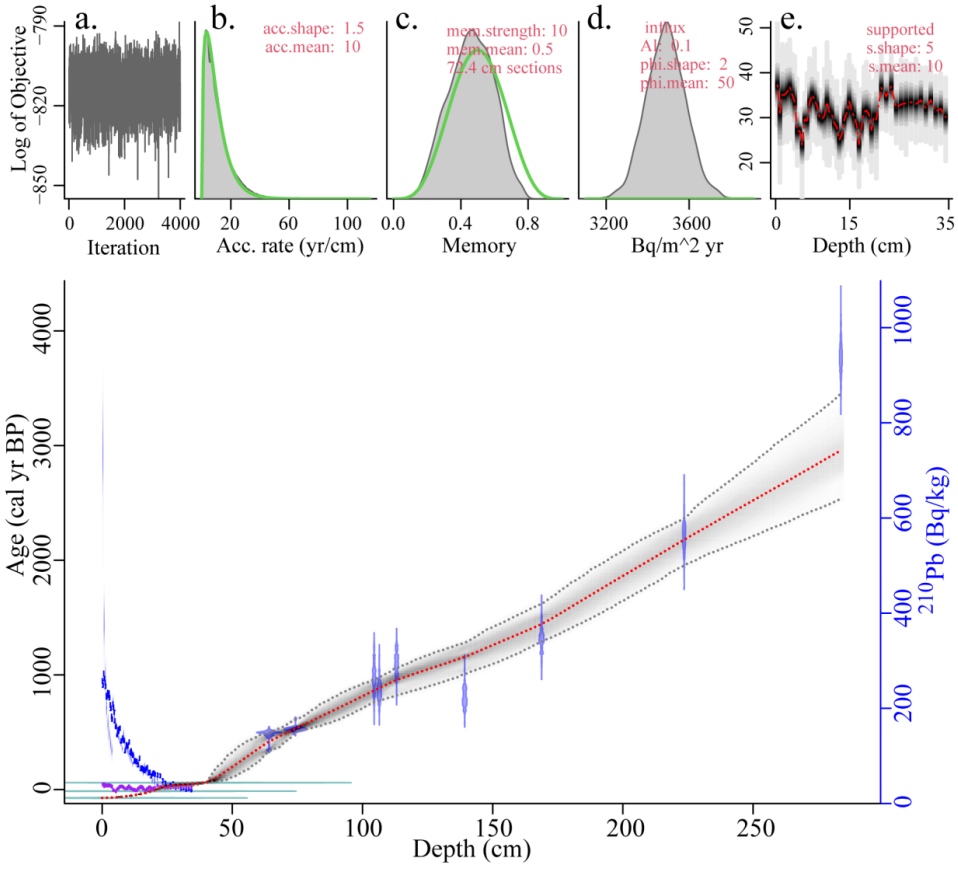


Figure 3. Bayesian age–depth model for the Lake Bullen Merri composite record. Pale blue markers depict probability distributions for radiocarbon-dated samples against the age axis (left). Small rectangles indicate the total (dark blue) and supported (purple) ^{210}Pb activity against the Pb concentration axis (right), respectively. Green lines represent calendar ages assigned to the coring year, peak Pu concentration, and first appearance of *Pinus*. Grey dotted lines represent 95 % confidence intervals, with darker shading indicating the most likely ages. The red dotted line shows the weighted mean age. Upper panels show (a) the log-objective trace across Markov chain Monte Carlo (MCMC) iterations; prior (green) and posterior (grey) distributions for (b) accumulation rate (yr cm^{-1}), (c) memory function used to construct the model, (d) ^{210}Pb flux, and (e) posterior estimates of supported ^{210}Pb activity at each sampled sediment depth (Aquino-López et al., 2018; Blaauw and Christen, 2011).

3.3 Diatom assemblages

In total, 41 diatom taxa were identified from 248 sediment samples. All 41 taxa were included in the diatom stratigraphy and statistical analyses **(Fig. S4)**, while the 19 taxa that reached more than 7% relative abundance were plotted in Figure 4a. Taxa in Figure 4a are arranged according to their electrical

https://doi.org/10.5194/egusphere-2026-6649
Preprint. Discussion started: 13 November 2026
© Author(s) 2026. CC BY 4.0 License.

conductivity (EC) optima (Rahman et al., 2026) from left (high-EC, i.e. more saline) to right (low-EC, i.e. fresher). Zonation of the stratigraphy using CONISS defined nine major diatom assemblage zones (A–H) **(Fig. 4a)**, which were validated by the Broken Stick method **(Fig. S5)**. Changes in species abundance within these zones are interpreted as reflecting environmental changes in the lake through time.

Zone I (500 BCE–110 CE): characterised by a prolonged dominance of *Nitzschia frustulum*, with relative abundances of 84–98%. The near dominance over several centuries suggests that the lake had moderate and relatively stable salinity during this interval.

Zone H (110–380 CE): the dominance of *N. frustulum* declines gradually. At the same time, moderate-salinity taxa such as *Chaetoceros muelleri* increase to 34%, and saline taxa *Navicymbula pusilla* and *Tryblionella apiculata* reach 33% and 11%, respectively. Other saline taxa, including *Cocconeis placentula* and *Pinnunavis elegans* occur only at low abundances. The overall assemblage shift from *N. frustulum* towards these more saline and moderate-saline taxa indicates a transition toward higher salinity conditions compared with Zone I.

Zone G (380–760 CE): exhibits a pronounced alternation between saline and fresher taxa, indicating highly variable salinity. Saline taxa such as *Pinnunavis elegans* increase to 58%, while moderate-salinity *Chaetoceros muelleri* reaches 69%. At the same time, fresher taxa, particularly *Tabularia fasciculata*, attain abundances of up to 50%. This alternation of saline and freshwater indicators suggests that lake salinity fluctuated markedly during this period. Interpretation is partly constrained by a data gap between 555 and 680 CE, but the available samples clearly show oscillating salinity.

Zone F (760–880 CE): is dominated by freshwater taxa and reflects a low-salinity phase. *Tabularia fasciculata* reaches up to 80%, accompanied by *Staurosira construens* var. *venter* up to 19%, while saline taxa are present only in minor amounts. This assemblage composition indicates that lake water salinity decreased substantially and remained relatively low during this interval.

Zones E–D (880–1410 CE): these two zones broadly show similar species distributions and are characterised by a mixture of saline and fresher taxa, indicative of variable salinity. The most saline centric diatoms, *Cyclotella caspia* and *Cyclotella choctawhatcheeana*, appear and become abundant, reaching up to 12% and 45%, respectively. These saline tolerant species alternate with fresher diatoms such as the centric *Stephanocyclus meneghinianus* (up to 22%), and the pennate taxa *Tabularia fasciculata* (up to 56%) and *Staurosira construens* var. *venter* (up to 42%). This dynamic assemblage suggests repeated shifts between more saline and fresher conditions. Although zones E and D share a similar overall pattern, they are distinguished by the occurrence of *Pinnunavis elegans* and *Amphora commutata* in Zone D, which adds a distinctive saline component and justifies treating them as separate zones.

https://doi.org/10.5194/egusphere-2026-6649
Preprint. Discussion started: 13 November 2026
© Author(s) 2026. CC BY 4.0 License.

Zone C (1410–1650 CE): saline centric diatoms disappear and freshwater species dominate the assemblage. Among these fresher taxa, *Staurosira construens* var. *venter* reaches up to 35%, and *Amphora libyca* up to 21%. The absence of saline centric diatoms, combined with the strong dominance of freshwater taxa, marks one of the lowest salinity phases in the entire record.

Zone B (1650–1900 CE): records a renewed increase in salinity. The saline tolerant diatom *Cyclotella choctawhatcheeana* reappears and becomes dominant, reaching up to 68%. The saline pennate taxon *Navicymbula pusilla* also increases to 33%, while freshwater taxa co-occur but remain at relatively low abundances. This assemblage indicates that lake salinity rose again following the low-salinity conditions of Zone C, although some freshwater influence persisted.

Zone A (1900–2022 CE): represents the most recent interval and records the highest inferred salinity in the sequence. Centric taxa dominate the assemblage: *Cyclotella caspia* reaches up to 25% and *Cyclotella choctawhatcheeana* up to 86%. Pennate diatoms are rare, with proportions too low to be included in quantitative summaries. This overwhelming dominance of saline centric diatoms indicates that lake salinity has increased to its highest levels during the 20th and 21st centuries.

Diatom data from Tower Hill Main Lake are published in Mills et al. (2013) and Tyler et al. (2015) and presented in the supplementary material for clarity **(Fig. S6)**. Zonation of the stratigraphy using CONISS defined four major diatom assemblage zones (A–D), which were validated by the Broken Stick method **(Fig. S7)**. Diatom stratigraphic plots for Lake Elingamite and Lake Surprise are available in Barr et al. (2014) and are not reproduced here.

https://doi.org/10.5194/egusphere-2026-6649
Preprint. Discussion started: 13 November 2026
© Author(s) 2026. CC BY 4.0 License.

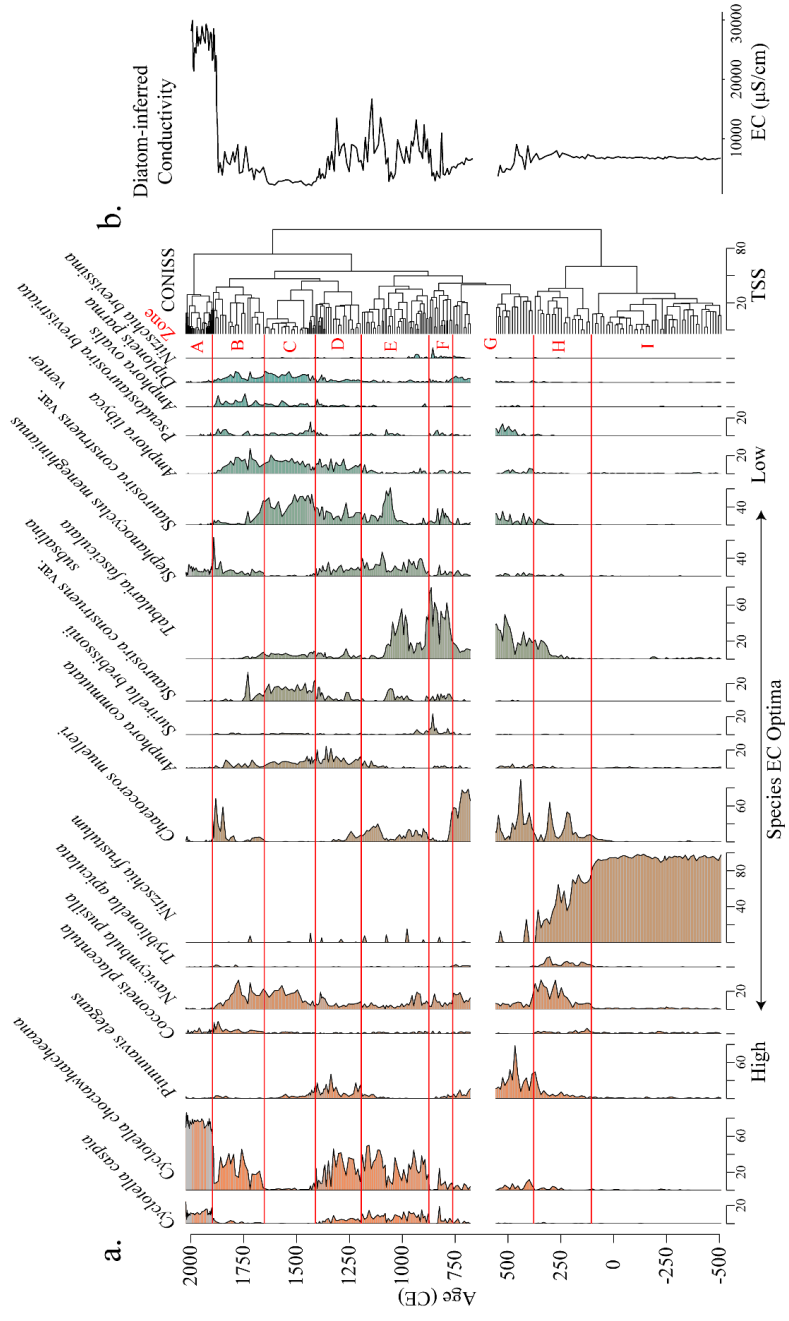


Figure 4. Diatom stratigraphy and reconstructed lake water conductivity for Lake Bullen Merri over the last 2500 years. (a) Diatom assemblages (>7% taxa) with CONISS zonation (zones A–H), taxa ordered by EC optima. TSS: Total sum of squares. (b) WA-based reconstruction of lake water EC showing temporal changes broadly corresponding to the assemblage zones.

https://doi.org/10.5194/egusphere-2026-6649
Preprint. Discussion started: 13 November 2026
© Author(s) 2026. CC BY 4.0 License.

3.4 Conductivity reconstructions

Past lake water conductivity-reconstructions for Lake Bullen Merri were generated using different methods (WA, WA-Inv, WA-Cla, LWWA-Inv, LWWA-Cla, WA-PLS) and all produced similar down-core trends over the last ~2500 years **(Fig. S8)**, indicating that the principal temporal patterns are robust to model selection. In the upper part of the core, after ~1890 CE, taxa with very high EC optima (e.g., *Cyclotella caspia* and *Cyclotella choctawhatcheeana*) are abundant. In this zone, deshrinking and WA-PLS-based methods counteract the inherent scale compression of simple WA, thereby yielding higher absolute EC estimates at the upper end of the calibration gradient (Birks, 1998; Liu et al., 2020). In this interval, simple WA reconstructs a maximum EC of 34,087 µS/cm, whereas the deshrinking and WA-PLS approaches yield higher maximum values, ranging from 49,362 µS/cm for WA-PLS component 2 to 115,494 µS/cm for WA-Cla (Supplementary datasets). Although all transfer-function approaches generate upper-core estimates above the modern measured EC range at Lake Bullen Merri (16,800–17,600 µS/cm; mean = 17,183 µS/cm), WA produces the lowest and comparatively closest estimates (~34,000 µS/cm). WA was therefore selected as the primary reconstruction **(Fig. 3b)**. However, our interpretations focus on temporal trends in reconstructed conductivity, which are similar across methods, rather than on absolute EC values.

Of the 41 fossil diatom taxa, 39 were represented in the Rahman et al. (2026) calibration dataset and had estimated EC optima. The two taxa (*Navicula tripunctata* and *Encyonema neomesianum*) absent from the calibration dataset occurred at low relative abundances. Taxa represented in the calibration dataset accounted for 94–100% of fossil diatom abundance in the sequence (mean = 99.8%), indicating generally high taxonomic coverage for the conductivity reconstructions. Reconstructed EC values for Lake Bullen Merri range from 2,139 to 34,087 µS/cm. On the basis of these reconstructed values, several distinct low-EC and high-EC periods can be identified over the last ~2500 years. These EC phases broadly align with diatom assemblage zones, although their boundaries do not coincide exactly because the zones reflect taxonomic turnover, whereas the EC phases reflect weighted ecological optima.

Over the earliest part of the record (from ~500 BCE to ~200 CE), reconstructed conductivity remained at intermediate levels during a prolonged interval dominated by *Nitzschia frustulum*, suggesting relatively stable, moderate salinity. After ~200 CE, the record is characterised by multi-century alternations between relatively high and low EC through the first and second millennia CE, forming several distinct cycles of rising and falling conductivity. During an overall period of higher EC in the late first and early second millennium CE, three marked cycles (~880–980 CE, ~1080–1200 CE, ~1250–1380 CE) are evident in which EC rose to pronounced peaks before returning to lower values, including a prolonged lower-EC interval from ~1380 to 1750 CE. From about 1890 to the present, reconstructed EC values increased sharply to their highest levels in the record, coincident with the

https://doi.org/10.5194/egusphere-2026-6649
Preprint. Discussion started: 13 November 2026
© Author(s) 2026. CC BY 4.0 License.

dominance of *Cyclotella caspia* and *Cyclotella choctawhatcheeana*, taxa with very high EC optima in the calibration dataset (Rahman et al., 2026). Because no samples could be analysed between ~555 and 680 CE, this interval cannot be clearly classified as either a low- or high-EC phase.

The same diatom–EC transfer function of Rahman et al. (2026) was also applied to diatom records from Lake Elingamite and Lake Surprise (Barr et al., 2014) and from Tower Hill Main Lake (Mills et al., 2013) to reconstruct their past EC history. Using this updated transfer function substantially improved the reconstructions for all sites, both in terms of absolute EC values and taxonomic coverage **(Fig. S9)**, yielding estimates that are more environmentally plausible. Across all these three additional records, sequences of relatively low and high EC broadly mirror the low- and high-EC phases of Lake Bullen Merri, indicating a regionally coherent pattern of salinity change.

4 Discussion

4.1 Electrical conductivity as an indicator of hydrologic change

Electrical conductivity (EC), a proxy for dissolved ion concentration, is widely used to characterise lake water salinity and to infer hydroclimatic variability in closed and semi-closed basins (Branchu and Bergonzini, 2004; Huybers et al., 2016; Steinman et al., 2013). In such systems, the water balance is governed by the interplay between precipitation, catchment runoff, groundwater inflow and evaporation (Compagnucci et al., 2001; Huybers et al., 2016). During wetter periods, increased precipitation and inflow raise lake level and water volume, diluting dissolved salts and reducing EC, whereas drier periods are characterised by reduced inflows and enhanced evaporative concentration, lowering lake level and increasing EC (Branchu and Bergonzini, 2004). This inverse lake level and salinity behaviour is a well-recognised feature of closed and semi-closed lakes and underpins the use of EC as a sensitive indicator of hydrologic and hydroclimatic change (Branchu and Bergonzini, 2004; Compagnucci et al., 2001; Steinman et al., 2013).

Modern observations and model results for Lake Bullen Merri demonstrate the applicability of Electrical Conductivity (EC) to characterise lake water salinity and to infer hydroclimate variability. Lake level and lake water EC or salinity show a pronounced inverse relationship (Ankor, 2020; Kirono et al., 2009). In 1889, lake level was approximately at 159 m AHD and modelled EC was ~9,000 µS/cm (Ankor, 2020). By December 1964 observed and modelled lake level had dropped to 147 m AHD (Jones et al., 2001) with mean EC increasing to 14,000 µS/cm in 1985 (Leahy, 2010). Salinity values of approximately 10 ppt (~16,000 µS/cm) were reported for 2008 (Kirono et al. 2009) and by 2018, lake level had declined to ~140 m AHD and measured EC was approximately 14,000 µS/cm (Ankor, 2020). Lake-water EC measured during field sampling in November 2023 reached its highest values at 17,183 µS/cm, when the lake level was approximately at 139 m AHD. These data demonstrate that a multi-decadal decline in lake level has been accompanied by a substantial increase in EC, consistent

https://doi.org/10.5194/egusphere-2026-6649
Preprint. Discussion started: 13 November 2026
© Author(s) 2026. CC BY 4.0 License.

with the expected response of closed-basin lakes to sustained hydrological deficits (Branchu and Bergonzini, 2004; Huybers et al., 2016; Steinman et al., 2013).

The modern climate at Lake Bullen Merri reinforces this sensitivity. Average annual rainfall in the catchment is around 775 mm, whereas mean annual evaporation is roughly 1250 mm (Ankor, 2020; Jeffrey et al., 2001), implying a long-term precipitation–evaporation deficit that favours evaporative concentration of dissolved salts. Hydrological modelling shows that the historical fall in water levels since the mid-1800s was initiated by a decrease in the precipitation/evaporation (P/E) ratio from a pre-1840 value of about 0.94–0.96 to a historical value of ~0.79 (Jones et al., 2001). Future climate scenarios project further declines in P/E, a continuously falling lake level, and a rise in salinity from the present brackish state toward approximately 20 ppt (~32,000 µS/cm) by 2100 (Kirono et al., 2009). Together, these results show that modest but sustained changes in P/E can drive large, long-term changes in both lake level and salinity.

These modern observations underpin our use of EC as a quantitative hydroclimatic proxy for the sediment record from Lake Bullen Merri. As EC responds predictably to the integrated effects of precipitation and evaporation, higher inferred lake water EC is interpreted to be representative of episodes of sustained drying and lake-level decline, whereas lower EC indicates intervals of increased effective precipitation, rising lake levels and dilution. On this basis, reconstructed EC from diatoms serves not only as a descriptor of past water chemistry but also as a robust indicator of hydrologic change and hydroclimate variability, allowing Lake Bullen Merri to contribute meaningfully to regional reconstructions of hydroclimate over the last ~2500 years.

4.2 Hydroclimate variability over the last ~2500 years

Several multidecadal- to centennial-scale dry and wet phases are identified over the last ~2500 years **(Fig. 5a)** from the diatom-based salinity reconstruction of Lake Bullen Merri. For the initial centuries (~500 BCE to ~200 CE), reconstructed EC suggests relatively stable, moderate salinity in Lake Bullen Merri, although this interval must be interpreted with caution because the diatom assemblage is dominated by a single taxon, *Nitzschia frustulum*. This taxon is widely regarded as a benthic species with a preference for alkaline waters with moderate to high conductivity, and can reach very high relative abundances in brackish–saline systems, including nearly 70% of the assemblage at chloride concentrations of 1000–2500 mg/L where it is grouped with halophilous taxa (Coring and Bäthe, 2011; Kociolek and Herbst, 1992; Lengyel et al., 2015; Trobajo et al., 2011). Ecological indicator values from a large-scale synthesis of diatom preferences from freshwater, brackish and marine waters in The Netherlands, characterise *N. frustulum* as an alkaliphilous taxon associated with slightly saline to low-end brackish (salinity ~0.9–1.8 ‰) and eutrophic waters, with moderate organic enrichment (Van Dam et al., 1994; Mertens et al., 2025). In the Rahman et al. (2026) calibration dataset from south-eastern Australia, *N. frustulum* occurred in 143 of 475 samples and reached a maximum relative abundance of

https://doi.org/10.5194/egusphere-2026-6649
Preprint. Discussion started: 13 November 2026
© Author(s) 2026. CC BY 4.0 License.

43.2% in Lake Linlithgow, which is a very shallow, saline (7038–13,970 µS/cm), alkaline (pH 8.3–9.9), and turbid lake. Its weighted-average EC optimum was 6,811 µS/cm, indicating an association with moderately saline waters. The taxon was also associated with alkaline conditions in the dataset (weighted-average pH = 8.45). A previous palaeolimnological study of Lake Bullen Merri similarly identified intervals (1,850–150 BCE) with *N. frustulum* reaching 100% relative abundance, which were interpreted as representing periods of much lower salinity than present (Duthie, 2000). Taken together, these lines of evidence suggest that the long interval dominated by *N. frustulum* in the early CE most likely represents a persistently alkaline, moderately saline, nutrient-rich lake with good oxygenation and productive benthic habitats. However, because the assemblage is nearly monospecific and *N. frustulum* has a broad ecological tolerance, it offers limited leverage for resolving more subtle hydrological differences. Therefore, we cannot subdivide this interval into discrete dry or wet phases.

Following the long *Nitzschia* dominated interval, the Lake Bullen Merri record indicates a relatively dry period from ~200–460 CE, during which salinity increased, and lake level declined. This is followed by a short-wet phase from ~460–555 CE, marked by fresher conditions and higher inferred lake levels, and then a dry phase from ~680–750 CE, when salinity again rose and lake level fell. We cannot fully resolve the period between ~555 and 680 CE. However, it most likely represents a transition between the preceding wet phase and the subsequent dry phase rather than a separate, well-defined state.

From the late first millennium into the early second millennium CE, the record shows three cycles of alternating salinity, and thus, wet and dry phases. Wet phases occur around ~750–880, ~980–1080 and ~1200–1250 CE, when lower EC and higher lake levels indicate wetter conditions. These are separated by drier phases around ~880–980, ~1080–1200 and ~1250–1380 CE, when higher EC and lower lake levels indicate reduced effective moisture. Together, these shifts demonstrate repeated multi-decadal swings between more humid and more arid conditions in south-eastern Australia.

At the end of these centennial scale cycles, the record shifts into a prolonged wet phase between ~1380 and ~1750 CE, during which inferred EC values are at their lowest sustained levels, implying persistently fresh conditions and high lake levels over several centuries. This wet interval broadly overlaps with the Little Ice Age (LIA) and is followed by a gradual drying trend, consistent with the wet LIA and post-LIA drying proposed by Tibby et al. (2018). The prominent wet phase at Lake Bullen Merri ends earlier than the 1850–1900 CE interval identified by Tibby et al. (2018) and is instead characterised by slightly higher EC between 1750–1890 CE. This signal also contrasts with the observations of lake overflow in 1841 CE (Currey, 1970). However, this particular event may correspond with a short but notable decline in inferred EC in the late 1800s, associated with a clear decline in the saline taxa *C. choctawhatcheeana* and *Chaetoceros muelleri* and an increase in the freshwater diatoms *Pseudostaurosira brevistriata* and *Amphora ovalis*. Beyond this, the lake enters a phase of very high inferred salinity, that likely reflects a combination of climatic drying and

https://doi.org/10.5194/egusphere-2026-6649
Preprint. Discussion started: 13 November 2026
© Author(s) 2026. CC BY 4.0 License.

anthropogenic impact. This late interval coincides with the appearance of exotic *Pinus* pollen and a marked shift in diatom assemblages, consistent with land-use change in the catchment. Consequently, the high-salinity phase after ~1890 CE is interpreted in the context of both climate-driven and anthropogenic salinity change. At a broader regional scale, although multi-year droughts are a natural feature of Australian hydroclimate, climate-model simulations suggest that the tendency towards longer droughts in eastern Australia during the twentieth century may indicate an emerging anthropogenic influence, consistent with projected declines in cool-season rainfall across southern Australia (Falster et al., 2024).

The extent to which the Bullen Merri record is representative of regional-scale hydroclimate change was evaluated through comparison with three other diatom records from crater lakes in western Victoria. Reconstructed EC from the Tower Hill Main Lake diatom record **(Fig. 5b)**, together with updated EC reconstructions from Lake Elingamite **(Fig. 5c)** and Lake Surprise **(Fig. 5d)**, show periods of alternating higher (drier) and lower EC (wetter) phases. Despite limited age control for Tower Hill and Elingamite records, the three sequences display broadly similar hydroclimatic trends compared to the Lake Bullen Merri record. This agreement between nearby crater lakes strengthens the hydroclimatic reconstruction and suggests a coherent pattern of hydroclimate variability within the maar-lake region of south-eastern Australia over much of the last ~2500 years. This has previously been suggested by Tyler et al. (2015), who showed that decadal resolved diatom records from western Victoria can capture coherent regional-scale environmental patterns. Collectively, these four records demonstrate higher effective precipitation over evaporation (P/E) during the LIA and, with less certainty, pronounced dry intervals during the preceding Medieval Climate Anomaly. The magnitude of these changes was substantial: a doubling of salinity at Lake Bullen Merri implies a considerable fall in lake level, and at Lake Elingamite reconstructed EC at ~1350 CE was approximately three times higher than at ~1750 CE. Such shifts would have had major consequences for lake ecology and illustrate a highly variable regional hydroclimate.

In contrast to this internal coherence, all four diatom records differ markedly from the 'canonical' lake-level reconstruction for Lake Keilambete (Bowler and Hamada, 1971; Wilkins et al. 2013), located less than 25 km NW of Lake Bullen Merri. This may relate to a chronological issue. As noted by Tibby et al. (2018), the Lake Keilambete record does not have a reliable chronology for the uppermost sediments, and a portion of that record may even be missing, which in turn affects the deeper sediment chronology. The substantially lower temporal resolution of this record may also fail to capture the finer scale hydroclimatic variability identified at Lake Bullen Merri. In addition, the Lake Keilambete lake level reconstruction is based on an inverse exponential relationship between lake water depth and the proportion of sediment retained in a 63 µm sieve. While this proxy could be interpreted to reflect changes in lake level due to a slightly increased catchment with erosion during low lake levels, the authors note that the data should be treated with caution for reasons such as non-linear responses of

https://doi.org/10.5194/egusphere-2026-6649
Preprint. Discussion started: 13 November 2026
© Author(s) 2026. CC BY 4.0 License.

Lake Keilambete to high water levels and radiocarbon reservoir anomalies from groundwater (Wilkins et al., 2013) **(Fig. S10e)**.

Extending the comparison further to the east, a water-table reconstruction using testate amoebae from Snowy Flat Wetland, Australian Capital Territory, shows broadly similar hydroclimatic trends to Lake Bullen Merri. In particular, the site records two cycles of alternating wet and dry conditions between approximately 680 and 1100 CE. A pronounced dry phase followed, lasting until approximately 1300 CE. A subsequent wet period persisted until the 19th century, followed by relatively dry conditions (Zheng et al., 2025) **(Fig. S10.f)**. This pattern also supports the hypothesis of a wet LIA followed by drying. In contrast, the pigment-inferred precipitation record from Rebecca Lagoon, Tasmania (Saunders et al., 2012) exhibits less resemblance to the Lake Bullen Merri EC record, except for predominantly wetter conditions during the LIA, at least until ~1500 CE **(Fig. S10.g)**. Magnesium concentrations in a stalagmite at Kubla Khan Cave, Tasmania, interpreted to reflect hydroclimate, exhibit similar hydroclimatic trends like Lake Bullen Merri over the last millennium and in parts of the first millennium CE, albeit limited by a relatively low ~50-year sampling resolution (Cooley et al., 2026) **(Fig. S10.h)**. Thus, all three records indicate a predominantly wetter phase in south-eastern Australia during the LIA, although its timing differs between sites. The Victorian diatom-based reconstructions were also compared with two records from South Australia to the west of Lake Bullen Merri. A bivalve $\delta^{18}O$ record from the Coorong Lagoon **(Fig. S10i**; Chamberlayne et al., 2023) and an ostracod $\delta^{18}O$ record from Lashmars Lagoon **(Fig. S10j;** Rahman et al., 2025). Both show sequences of dry and wet periods, but the timing and expression of these phases largely differ from the Victorian diatom-based EC records. In all cases, chronological imprecision hinders the direct comparison of sub-centennial scale variability, however it is clear that a variety of different sedimentary environments record notable decadal- and centennial-scale hydroclimatic extremes, illustrating the prevalence of such events in the Australian climate system.

Tree-ring-based hydroclimate records from Australia typically have more limited temporal coverage than the Bullen Merri record. A single tree-ring chronology derived from climatically connected regions, interpreted to reconstruct winter streamflow of the Murray River, extends back to 1190 CE (Higgins et al., 2023). This record of Murray River inflow which shares climate drivers with our study region (Risbey et al., 2009) suggests prolonged early-thirteenth-century droughts that overlap with the final dry phase inferred at Bullen Merri between approximately 1250 and 1380 CE. However, this tree ring-based reconstruction do not consistently indicate a prolonged wet phase during the LIA, in contrast to the persistently low EC at Bullen Merri and other crater lakes from approximately 1380 to 1750 CE, which likely reflects sustained high effective moisture. Although Freund et al. (2017) and Higgins et al. (2023) identify the Millennium Drought as exceptionally extensive and severe within their respective reconstruction periods, these records do not extend far enough back in time to evaluate whether the earlier prominent dry phases inferred at Bullen Merri, particularly before 1190 CE, were of comparable

https://doi.org/10.5194/egusphere-2026-6649
Preprint. Discussion started: 13 November 2026
© Author(s) 2026. CC BY 4.0 License.

or greater severity. Similarly, shorter reconstructions from tree ring records that aim to infer climate from our study region (i.e. the "southern slopes" natural resource management region cluster) do not identify a distinctly wet LIA (Freund et al., 2017; Palmer et al., 2024).

Antarctic ice-core data provide longer records comparable to that from Lake Bullen Merri. Several studies infer rainfall variability in Australia based on statistical relationships between ice accumulation and summer sea salt deposition at Law Dome, East Antarctica (Van Ommen and Morgan, 2010; Roberts et al., 2015; Tozer et al., 2016; Vance et al., 2013, 2015). The Law Dome summer sea salt record was used to infer a prolonged dry interval between approximately 1000 and 1260 CE, including a 39-year drought in eastern Australia from 1174 to 1212 CE (Vance et al., 2013). These intervals broadly overlap with the Bullen Merri dry phase from approximately 1080 to 1200 CE and the transition to another dry phase after approximately 1250 CE. The sustained low EC at Bullen Merri between approximately 1380 and 1750 CE broadly overlaps with wetter conditions inferred from the Law Dome-derived eastern Australian rainfall records. Vance et al. (2013) identified a generally wetter interval from approximately 1260 to 1860 CE, although this period included shorter dry episodes. Importantly, the prolonged dry conditions prior to 1200 CE are not reflected in summer sea salt at Law Dome (Roberts et al., 2015). In contrast, the wetter pre-late-nineteenth-century conditions reported for eastern Australia by Tibby et al. (2018) are present in all these records, including a wetter interval extending to approximately 1860 CE in Vance et al. (2013). Because the Law Dome inferred rainfall reconstructions are based on statistical relationships with instrumental data of eastern Australian rainfall, the strength and spatial expression of these relationships may have varied through time. Consequently, these comparisons should be interpreted cautiously.

While the four Victorian crater lake diatom-inferred EC records exhibit similar patterns, comparison with more distant records suggest greater spatial and temporal variability across south-eastern Australia. This may reflect real differences in moisture source, catchment setting, and hydrology, differences between the proxies themselves, or chronological uncertainties. For example, speleothem trace-elements, bivalve $\delta^{18}O$, and ostracod $\delta^{18}O$ records are sensitive to seasonal and interannual hydroclimate variability, whereas lake water salinity integrates the balance of precipitation, evaporation, inflow, and groundwater exchange over several years. In addition, differences in chronological precision as well as in variable temporal smoothing of sediment records may result in amplification of low frequency variability at the expense of short-term patterns. Less agreement between different palaeoclimate records is therefore not unexpected and does not indicate that any one record is unreliable. Importantly, the similar trends between records suggest that the shared pattern is unlikely to be an artefact of proxy behaviour, of local conditions or of applied age models.

These records also refine how CE hydroclimate in south-eastern Australia is understood. Annually resolved reconstructions from tree rings, corals, and ice cores are mostly interpreted at interannual to

https://doi.org/10.5194/egusphere-2026-6649
Preprint. Discussion started: 13 November 2026
© Author(s) 2026. CC BY 4.0 License.

multidecadal scales (e.g. Freund et al., 2017; Higgins et al., 2023; Palmer et al., 2024). Where century-long wet or dry periods have been identified, they appear as shifts of relatively small amplitude compared with the large-scale changes in effective moisture indicated by diatom records. Although sediment mixing can attenuate high-frequency variability in lake sediment records and make low-frequency signals relatively more prominent, this is unlikely for the crater lakes given their rapid accumulation rates, particularly at Lake Surprise, and the occurrence of similar trends in four separate sequences. An explanation may instead lie in how the annually resolved reconstructions are constructed. Tree-ring standardisation and calibration against relatively short instrumental records can reduce low-frequency variance in hydroclimatic reconstructions (Cook et al., 1995; Ljungqvist et al., 2020; Von Storch et al., 2004). Available tree-ring records provide limited coverage of the early first millennium CE and therefore limited representation of the pronounced dry conditions inferred at Lake Bullen Merri during the medieval period. This comparison provides a site-specific long-term context for natural effective-moisture variability, providing essential context for water-resource planning alongside projections of anthropogenic climate change.

The centennial-scale hydroclimatic variability identified at Lake Bullen Merri likely reflects interactions among large-scale climate modes, synoptic rainfall-producing systems, and land–atmosphere feedbacks, rather than a single driver (Holgate et al., 2025; McKay et al., 2023). El Niño–Southern Oscillation, the Indian Ocean Dipole, and the Southern Annular Mode can modulate moisture transport and rainfall-producing circulation over south-eastern Australia in spatially and seasonally variable ways, while soil-moisture, evapotranspiration, and precipitation-recycling feedbacks may affect the persistence of wet and dry conditions (Holgate et al., 2020, 2025; McKay et al., 2023). The diatom-inferred EC record integrates the balance between precipitation and evaporation and cannot distinguish whether the centennial-scale phases at Lake Bullen Merri were driven primarily by changes in rainfall, evaporative stress, or both. The sustained low salinity and high inferred lake levels during the LIA may be consistent with reduced evaporative demand under cooler conditions, and this interpretation gains some support from the association between large volcanic eruptions and drought-free intervals in the Murray–Darling Basin identified by Falster et al. (2024), which was attributed to aerosol cooling suppressing evaporative demand. Testing this hypothesis requires temperature reconstructions of comparable resolution and length, and these are not presently available for south-eastern Australia. Regional temperature reconstructions for Australasia rely on only three records from before 1400 CE (Gergis et al., 2016), and there is little evidence that warm and cold epochs of the Common Era were globally or hemispherically synchronous (Anchukaitis et al., 2017; Neukom et al., 2019). Whether the Medieval Climate Anomaly was warm across the Southern Hemisphere and the Indian and Pacific basins therefore remains uncertain. Resolving the relative contributions of precipitation and evaporation to the variability reported here will require independent, well-dated temperature proxies from the same or nearby sites, ideally applied to the same sediment sequences.

https://doi.org/10.5194/egusphere-2026-6649
Preprint. Discussion started: 13 November 2026
© Author(s) 2026. CC BY 4.0 License.

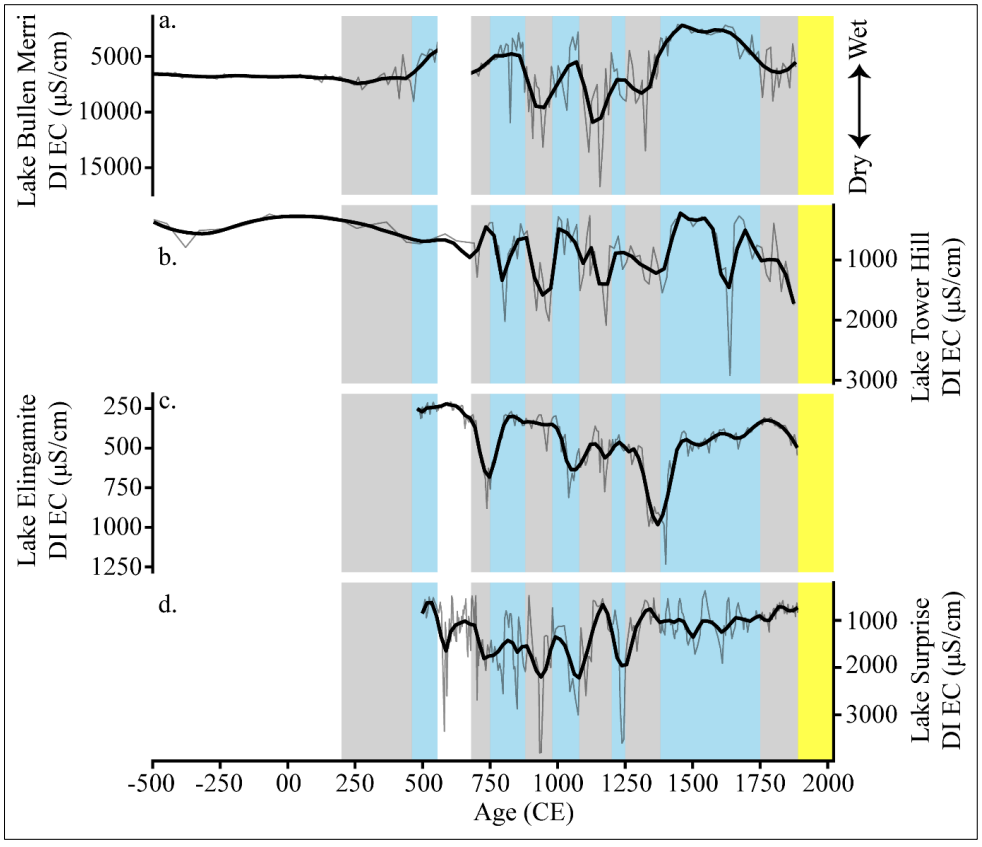


Figure 5. Comparison of diatom-inferred (DI) EC records reconstructing hydroclimate variability from **a.** Lake Bullen Merri, **b.** Lake Tower Hill (Mills et al., 2013), **c.** Lake Elingamite, and **d.** Lake Surprise (c–d; Barr et al., 2014). Yellow panel marks the interval interpreted as strongly influenced by anthropogenic impact. Grey and blue bars indicate dry and wet periods, respectively, while the white bar indicates a gap in the record. Black lines indicate a locally weighted sum of squares (loess) fit with span = 0.1 (Cleveland et al., 2017).

5 Conclusions

We derived a ~2500 years diatom-based EC record to infer hydroclimate variability at Lake Bullen Merri, Victoria. Relatively stable, moderate salinity characterised the interval from ~500 BCE to ~200 CE. EC then rose and fluctuated between ~200 and ~750 CE, before varying through three further wet–dry cycles between ~750 and ~1380 CE. A prolonged freshwater phase followed between ~1380 and ~1750 CE, coinciding with the LIA, when reconstructed EC was lowest and saline centric diatoms were absent. EC rose again to ~1890 CE and reached its highest values thereafter; the coincidence of this

https://doi.org/10.5194/egusphere-2026-6649
Preprint. Discussion started: 13 November 2026
© Author(s) 2026. CC BY 4.0 License.

shift with exotic *Pinus* pollen indicates that anthropogenic catchment disturbances contributed alongside climatic drying.

Comparable reconstructions from Lake Tower Hill, Lake Elingamite and Lake Surprise show broadly similar phases, indicating that these lakes recorded a shared regional hydroclimatic signal rather than site-specific changes. Reconstructed EC at Lake Bullen Merri roughly doubled between the wettest and driest phases of the last millennium, a large change that altered lake level and lake ecology. These centennial-scale phases are not clearly expressed in regional tree-ring and ice-core-derived reconstructions, which are shorter and differently calibrated. Therefore, the diatom records indicate a wider natural range of hydroclimatic variability than currently recognised. This further suggests that water resource risk assessments derived from tree-ring and ice-core records are likely to underestimate the hazards posed by natural droughts.

Data availability

The original data used in this study are available as part of the downloadable Supplement accompanying this manuscript.

Author contributions

MR: Conceptualization, Fieldwork, Laboratory analyses, Formal analysis, Writing – original draft, Visualization**. KE:** Fieldwork, Laboratory analyses, Writing – review & editing. **ÖK:** Laboratory analyses, Writing – review & editing. **WT:** Fieldwork, Laboratory analyses, Writing – review & editing. **BZ:** Fieldwork, Laboratory analyses, Writing – review & editing, Funding acquisition. **KM:** Resources, Writing – review & editing. **VM:** Laboratory analyses, Writing – review & editing. **HC:** Fieldwork, Writing – review & editing. **MA:** Resources, Writing – review & editing. **CB:** Resources, Writing – review & editing. **AF:** Fieldwork, Writing – review & editing. **DC:** Laboratory analyses, Writing – review & editing. **GJ:** Laboratory analyses, Writing – review & editing. **MH:** Laboratory analyses, Writing – review & editing. **JT:** Conceptualization, Formal analysis, Writing – review & editing. **JonT:** Conceptualization, Fieldwork, Formal analysis, Writing – review & editing, Funding acquisition.

Competing interests

The authors have the following competing interests: At least one of the (co-)authors is a member of the editorial board of Climate of the Past.

Disclaimer

Publisher's note: Copernicus Publications remains neutral with regard to jurisdictional claims made in the text, published maps, institutional affiliations, or any other geographical representation in this paper. The authors bear the ultimate responsibility for providing appropriate place names. Views expressed in the text are those of the authors and do not necessarily reflect the views of the publisher.

https://doi.org/10.5194/egusphere-2026-6649
Preprint. Discussion started: 13 November 2026
© Author(s) 2026. CC BY 4.0 License.

Acknowledgements

We would like to express our sincere thanks to Professor Peter A. Gell for his cooperation in identifying diatoms and for confirming our diatom identifications. We acknowledge the financial support from the Australian Government for the Centre for Accelerator Science at ANSTO through the National Collaborative Research Infrastructure Strategy (NCRIS). We acknowledge the Eastern Maar Peoples as the Traditional Owners and custodians of the lands and waters on which Lake Bullen Merri is located and pay our respects to their Elders past and present. The authors acknowledge the use of Perplexity AI to assist with language editing and improve the clarity of the manuscript; all suggested revisions were reviewed by the authors.

Financial support

This research was supported by an Australian Research Council (ARC) Future Fellowship awarded to Jonathan Tyler (FT230100648) and a German Research Foundation (DFG) research grant awarded to Bernd Zolitschka and Özlem Karadas (grant no. 457251753). Radiocarbon dating and plutonium isotope analyses conducted at the Centre for Accelerator Science, ANSTO, were funded by ANSTO grant AP18268.

References

Anchukaitis, K. J., Wilson, R., Briffa, K. R., Büntgen, U., Cook, E. R., D'Arrigo, R., Davi, N., Esper, J., Frank, D., Gunnarson, B. E., Hegerl, G., Helama, S., Klesse, S., Krusic, P. J., Linderholm, H. W., Myglan, V., Osborn, T. J., Zhang, P., Rydval, M., Schneider, L., Schurer, A., Wiles, G., and Zorita, E.: Last millennium Northern Hemisphere summer temperatures from tree rings: Part II, spatially resolved reconstructions, Quat. Sci. Rev., 163, 1–22, https://doi.org/10.1016/j.quascirev.2017.02.020, 2017.

Ankor, M. J.: Hydrologic and Isotopic Lake Modelling for Palaeoclimate Research, Doctoral dissertation. University of Adelaide, 2020.

Aquino-López, M. A., Blaauw, M., Christen, J. A., and Sanderson, N. K.: Bayesian analysis of 210 Pb dating, J. Agric. Biol. Environ. Stat., 23, 317–333, https://doi.org/10.1007/s13253-018-0328-7, 2018.

Armstrong, M. S., Kiem, A. S., and Vance, T. R.: Comparing instrumental, palaeoclimate, and projected rainfall data: Implications for water resources management and hydrological modelling, J. Hydrol. Reg. Stud., 31, 100728, https://doi.org/10.1016/J.EJRH.2020.100728, 2020.

Australian Academy of Technological Sciences and Engineering.: Exotic pines, in: Engineering, A.A. of T.S. and (Ed.), Technology in Australia 1788–1988. Melbourne, p. 210, 1988.

Babst, F., Bodesheim, P., Charney, N., Friend, A. D., Girardin, M. P., Klesse, S., Moore, D. J. P., Seftigen, K., Björklund, J., and Bouriaud, O.: When tree rings go global: Challenges and opportunities

https://doi.org/10.5194/egusphere-2026-6649
Preprint. Discussion started: 13 November 2026
© Author(s) 2026. CC BY 4.0 License.



for retro-and prospective insight, Quat. Sci. Rev., 197, 1–20, https://doi.org/10.1016/j.quascirev.2018.07.009, 2018.

Barr, C., Tibby, J., Gell, P., Tyler, J., Zawadzki, A., and Jacobsen, G. E.: Climate variability in south-eastern Australia over the last 1500 years inferred from the high-resolution diatom records of two crater lakes, Quat. Sci. Rev., 95, 115–131, https://doi.org/10.1016/j.quascirev.2014.05.001, 2014.

Barr, C.: Droughts and flooding rains: a fine-resolution reconstruction of climatic variability in Western Victoria, Australia, over the last 1500 years, Doctoral dissertation. University of Adelaide, 2010.

Battarbee, R. W.: Palaeolimnological approaches to climate change, with special regard to the biological record, Quat. Sci. Rev., 19, 107–124, https://doi.org/10.1016/S0277-3791(99)00057-8, 2000.

Battarbee, R. W., Jones, V. J., Flower, R. J., Cameron, N. G., Bennion, H., Carvalho, L., and Juggins, S.: Diatoms, in: Tracking environmental change using lake sediments: terrestrial, algal, and siliceous indicators, Springer, 155–202, https://doi.org/10.1007/0-306-47668-1_8, 2001.

Bennett, K. D.: Determination of the number of zones in a biostratigraphical sequence, New Phytol., 132, 155–170, https://doi.org/10.1111/j.1469-8137.1996.tb04521.x, 1996.

Bird, B. W., Abbott, M. B., Vuille, M., Rodbell, D. T., Stansell, N. D., and Rosenmeier, M. F.: A 2,300-year-long annually resolved record of the South American summer monsoon from the Peruvian Andes, Proc. Natl. Acad. Sci., 108, 8583–8588, https://doi.org/10.1073/pnas.1003719108, 2011.

Birks, H. H.: Ecological responses to late-glacial climate changes in northern and western Norway, Quat. Int., 279, 52, 2012.

Birks, H. J. B.: Numerical tools in palaeolimnology: progress, potentialities, and problems, J. Paleolimnol., 20, 307–332, https://doi.org/10.1016/j.quaint.2012.07.227, 1998.

Blaauw, M. and Christen, J. A.: Flexible paleoclimate age-depth models using an autoregressive gamma process, 6 (3) 457 – 474, https://doi.org/10.1214/11-BA618, 2011.

Blinn, D. W.: Diatom community structure along salinity gradients in Australia saline lakes: biogeographic comparisons with other continents, in: A Century of Diatom Research in North America. Special Symposium for Reimer and Patrick Festschrift. Koeltz Scientific Books, 163–174, https://www.amazon.sg/Century-Diatom-Research-North-America/dp/1878762753, 1995.

Branchu, P. and Bergonzini, L.: Chloride concentrations in Lake Tanganyika: an indicator of the hydrological budget?, Hydrol. Earth Syst. Sci., 8, 256–265, https://doi.org/10.5194/hess-8-256-2004, 2004.

Cadd, H., Sherborne-Higgins, B., Becerra-Valdivia, L., Tibby, J., Barr, C., Forbes, M., Cohen, T. J., Tyler, J., Vandergoes, M., and Francke, A.: The application of pollen radiocarbon dating and bayesian

https://doi.org/10.5194/egusphere-2026-6649
Preprint. Discussion started: 13 November 2026
© Author(s) 2026. CC BY 4.0 License.

age-depth modeling for developing robust geochronological frameworks of wetland archives, Radiocarbon, 64, 213–235, https://doi:10.1017/RDC.2022.29, 2022.

Chamberlayne, B. K., Tyler, J. J., Haynes, D., Shao, Y., Tibby, J., and Gillanders, B. M.: Hydrological change in southern Australia over 1750 years: a bivalve oxygen isotope record from the Coorong Lagoon, Clim. Past, 19, 1383–1396, https://doi.org/10.5194/cp-19-1383-2023, 2023.

Chambers, J. W. and Cameron, N. G.: A rod-less piston corer for lake sediments; an improved, rope-operated percussion corer, J. Paleolimnol., 25, 117–122, https://doi.org/10.1023/A:1008181406301, 2001.

Child, D. P., Hotchkis, M. A. C., and Williams, M. L.: High sensitivity analysis of plutonium isotopes in environmental samples using accelerator mass spectrometry (AMS), J. Anal. At. Spectrom., 23, 765–768, https://doi.org/10.1039/b715788f, 2008.

Cleveland, W. S., Grosse, E., and Shyu, W. M.: Local regression models, in: Statistical models in S, Routledge, 309–376, https://doi.org/10.1201/9780203738535, 2017.

Compagnucci, R., da Cunha, L., Hanaki, K., Howe, C., Mailu, G., Shiklomanov, I., and Stakhiv, E.: Hydrology and water resources, in: Climate Change 2001: Impacts, Adaptation and Vulnerability, edited by: McCarthy, J. J., Canziani, O. F., Leary, N. A., Dokken, D. J., and White, K. S., Cambridge University Press, London, 191–233, https://www.ipcc.ch/site/assets/uploads/2018/03/wg2TARchap4.pdf, 2001.

Cook, B. I., Palmer, J. G., Cook, E. R., Turney, C. S. M., Allen, K., Fenwick, P., O'Donnell, A., Lough, J. M., Grierson, P. F., and Ho, M.: The paleoclimate context and future trajectory of extreme summer hydroclimate in eastern Australia, J. Geophys. Res. Atmos., 121, 12–820, https://doi.org/10.1002/2016JD024892, 2016.

Cook, B. I., Smerdon, J. E., Cook, E. R., Williams, A. P., Anchukaitis, K. J., Mankin, J. S., Allen, K., Andreu-Hayles, L., Ault, T. R., and Belmecheri, S.: Megadroughts in the Common Era and the Anthropocene, Nat. Rev. Earth Environ., 3, 741–757, https://doi.org/10.1038/s43017-022-00329-1, 2022.

Cook, E. R., Briffa, K. R., Meko, D. M., Graybill, D. A., and Funkhouser, G.: The'segment length curse'in long tree-ring chronology development for palaeoclimatic studies, The Holocene, 5, 229–237, https://doi.org/10.1177/095968369500500211, 1995.

Cooley, S. R., Fletcher, M.-S., Drysdale, R. N., MacGregor, C., Treble, P. C., Hua, Q., Hellstrom, J., Demény, A., Greig, A., and Eberhard, R.: Holocene hydroclimate, fire, and the persistence of coniferous sub-alpine rainforest in Tasmania, Australia, Quat. Sci. Rev., 384, 109996, https://doi.org/https://doi.org/10.1016/j.quascirev.2026.109996, 2026.

https://doi.org/10.5194/egusphere-2026-6649
Preprint. Discussion started: 13 November 2026
© Author(s) 2026. CC BY 4.0 License.



893 Coring, E. and Bäthe, J.: Effects of reduced salt concentrations on plant communities in the River Werra
894 (Germany), Limnologica, 41, 134–142, https://doi.org/https://doi.org/10.1016/j.limno.2010.08.004,
895 2011.

896 Currey, D. T.: Lake systems, Western Victoria, Aust. Soc. Limnol. Bull., 3, 1–13,
897 https://www.biodiversitylibrary.org/page/65169067#page/3/mode/1up, 1970.

898 D'Arrigo, R., Wilson, R., Liepert, B., and Cherubini, P.: On the 'divergence problem'in northern
899 forests: a review of the tree-ring evidence and possible causes, Glob. Planet. Change, 60, 289–305,
900 https://doi.org/10.1016/j.gloplacha.2007.03.004, 2008.

901 Van Dam, H., Mertens, A., and Sinkeldam, J.: A coded checklist and ecological indicator values of
902 freshwater diatoms from the Netherlands, Netherl. J. Aquat. Ecol., 28, 117–133,
903 https://doi.org/10.1007/BF02334251, 1994.

904 Dätwyler, C., Neukom, R., Abram, N. J., Gallant, A. J. E., Grosjean, M., Jacques-Coper, M., Karoly,
905 D. J., and Villalba, R.: Teleconnection stationarity, variability and trends of the Southern Annular Mode
906 (SAM) during the last millennium, Clim. Dyn., 51, 2321–2339, https://doi.org/10.1007/s00382-017-
907 4015-0, 2018.

908 De Deckker, P.: Holocene ostracods, other invertebrates and fish remains from cores of four maar lakes
909 in southeastern Australia, Proc. R. Soc. Victoria, 94, 183–220,
910 https://dn760004.eu.archive.org/0/items/biostor-259572/biostor-259572.pdf, 1982.

911 De Deckker, P. and Williams, W. D.: Physico-chemical limnology of eleven, mostly saline permanent
912 lakes in western Victoria, Australia, Hydrobiologia, 162, 275–286,
913 https://doi.org/10.1007/BF00016673, 1988.

914 Dharmarathna, A., Cadd, H., Barr, C., Francke, A., Hua, Q., Child, D., Hotchkis, M., Zawadzki, A.,
915 Gadd, P., and Turney, C.: Developing robust lake sediment chronologies using 210Pb, Pu and
916 radiocarbon dating of pollen concentrates and macrofossil: A case study from Lake Surprise, Victoria,
917 Australia, Quat. Geochronol., 89, 101686, https://doi.org/10.1016/j.quageo.2025.101686, 2025.

918 Dodson, J. R.: Late Pleistocene vegetation and environments near Lake Bullenmerri, western Victoria,
919 Aust. J. Ecol., 4, 419–427, https://doi.org/10.1111/j.1442-9993.1979.tb01570.x, 1979.

920 Duthie, T.: Nutrients in Pirron Yallock Creek, southwestern Victoria: paleolimnological and
921 management considerations, Master of Science Dissertation. Deakin University,
922 https://hdl.handle.net/10536/DRO/DU:30023517, 2000.

923 Duxbury, L. C., Haidee, C., Boone, L. W., Alexander, F., Stefan, C. L., Yohanni, J.-M. L., Anthony, H.
924 P., Linda, A., and James, T. J.: Long term context for bushfires in inhabited and uninhabited landscapes:

https://doi.org/10.5194/egusphere-2026-6649
Preprint. Discussion started: 13 November 2026
© Author(s) 2026. CC BY 4.0 License.

A Holocene record from Kangaroo Island (Karti/Karta), South Australia, Glob. Planet. Change, 105490, https://doi.org/10.1016/j.gloplacha.2026.105490, 2026.

Emile-Geay, J., McKay, N. P., Kaufman, D. S., von Gunten, L., Wang, J., Anchukaitis, K. J., Abram, N. J., Addison, J. A., Curran, M. A. J., Evans, M. N., Henley, B. J., Hao, Z., Martrat, B., McGregor, H. V, Neukom, R., Pederson, G. T., Stenni, B., Thirumalai, K., Werner, J. P., Xu, C., Divine, D. V, Dixon, B. C., Gergis, J., Mundo, I. A., Nakatsuka, T., Phipps, S. J., Routson, C. C., Steig, E. J., Tierney, J. E., Tyler, J. J., Allen, K. J., Bertler, N. A. N., Björklund, J., Chase, B. M., Chen, M.-T., Cook, E., de Jong, R., DeLong, K. L., Dixon, D. A., Ekaykin, A. A., Ersek, V., Filipsson, H. L., Francus, P., Freund, M. B., Frezzotti, M., Gaire, N. P., Gajewski, K., Ge, Q., Goosse, H., Gornostaeva, A., Grosjean, M., Horiuchi, K., Hormes, A., Husum, K., Isaksson, E., Kandasamy, S., Kawamura, K., Kilbourne, K. H., Koç, N., Leduc, G., Linderholm, H. W., Lorrey, A. M., Mikhalenko, V., Mortyn, P. G., Motoyama, H., Moy, A. D., Mulvaney, R., Munz, P. M., Nash, D. J., Oerter, H., Opel, T., Orsi, A. J., Ovchinnikov, D. V, Porter, T. J., Roop, H. A., Saenger, C., Sano, M., Sauchyn, D., Saunders, K. M., Seidenkrantz, M.-S., Severi, M., Shao, X., Sicre, M.-A., Sigl, M., Sinclair, K., St. George, S., St. Jacques, J.-M., Thamban, M., Kuwar Thapa, U., Thomas, E. R., Turney, C., Uemura, R., Viau, A. E., Vladimirova, D. O., Wahl, E. R., White, J. W. C., Yu, Z., Zinke, J., and Consortium, P.: A global multiproxy database for temperature reconstructions of the Common Era, Sci. Data, 4, 170088, https://doi.org/10.1038/sdata.2017.88, 2017.

Falster, G. M., Wright, N. M., Abram, N. J., Ukkola, A. M., and Henley, B. J.: Potential for historically unprecedented Australian droughts from natural variability and climate change, Hydrol. Earth Syst. Sci., 28, 1383–1401, https://doi.org/10.5194/hess-28-1383-2024, 2024.

Freund, M., Henley, B. J., Karoly, D. J., Allen, K. J., and Baker, P. J.: Multi-century cool- and warm-season rainfall reconstructions for Australia's major climatic regions, Clim. Past, 13, 1751–1770, https://doi.org/10.5194/cp-13-1751-2017, 2017.

Fritz, S. C., Juggins, S., Battarbee, R. W., and Engstrom, D. R.: Reconstruction of past changes in salinity and climate using a diatom-based transfer function, Nature, 352, 706–708, https://doi.org/10.1038/352706a0, 1991.

Gallant, A. J. E., Phipps, S. J., Karoly, D. J., Mullan, A. B., and Lorrey, A. M.: Nonstationary Australasian teleconnections and implications for paleoclimate reconstructions, J. Clim., 26, 8827–8849, https://doi.org/10.1175/JCLI-D-12-00338.1, 2013.

Gebregiorgis, D., Giosan, L., Hathorne, E. C., Anand, P., Nilsson-Kerr, K., Plass, A., Lückge, A., Clemens, S. C., and Frank, M.: What Can We Learn From X-Ray Fluorescence Core Scanning Data? A Paleomonsoon Case Study, Geochemistry, Geophys. Geosystems, 21, e2019GC008414, https://doi.org/10.1029/2019GC008414, 2020.

https://doi.org/10.5194/egusphere-2026-6649
Preprint. Discussion started: 13 November 2026
© Author(s) 2026. CC BY 4.0 License.

Gell, P. A.: The development of a diatom database for inferring lake salinity, western Victoria, Australia: towards a quantitative approach for reconstructing past climates, Aust. J. Bot., 45, 389–423, https://doi.org/10.1071/BT96036, 1997.

Gell, P. A.: Quantitative reconstructions of the Holocene palaeosalinity of paired crater lakes based on a diatom transfer function, Palaeoclimates, 3, 83–96, 1998.

Gell, P. A. and Gasse, F.: Relationships between salinity and diatom flora from some Australian saline lakes, Mem. Cal. Acad. Sci. 17, 631–647, 1994.

Gergis, J., Neukom, R., Gallant, A. J. E., and Karoly, D. J.: Australasian temperature reconstructions spanning the last millennium, J. Clim., 29, 5365–5392, https://doi.org/10.1175/JCLI-D-13-00781.1, 2016.

Gong, L., Lübbers, J., Beil, S., and Holbourn, A.: Data report: revised composite depth scale and splice for IODP Expedition 363 Site U1483, Proc. Int. Ocean Discov. Progr., 363, https://doi.org/10.14379/iodp.proc.363.201.2020, 2020.

Goodwin, I. D., Browning, S., Lorrey, A. M., Mayewski, P. A., Phipps, S. J., Bertler, N. A. N., Edwards, R. P., Cohen, T. J., van Ommen, T., and Curran, M.: A reconstruction of extratropical Indo-Pacific sea-level pressure patterns during the Medieval Climate Anomaly, Clim. Dyn., 43, 1197–1219, https://doi.org/10.1007/s00382-013-1899-1, 2014.

Gouramanis, C., Wilkins, D., and De Deckker, P.: 6000 years of environmental changes recorded in Blue Lake, South Australia, based on ostracod ecology and valve chemistry, Palaeogeogr. Palaeoclimatol. Palaeoecol., 297, 223–237, https://doi.org/10.1016/j.palaeo.2010.08.005, 2010.

Grimm, E. C.: CONISS: a FORTRAN 77 program for stratigraphically constrained cluster analysis by the method of incremental sum of squares, Comput. Geosci., 13, 13–35, https://doi.org/10.1016/0098-3004(87)90022-7, 1987.

Hancock, G. J., Leslie, C., Everett, S. E., Tims, S. G., Brunskill, G. J., and Haese, R.: Plutonium as a chronomarker in Australian and New Zealand sediments: a comparison with 137Cs, J. Environ. Radioact., 102, 919–929, https://doi.org/10.1016/j.jenvrad.2009.09.008, 2011.

Harrison, J. J., Saunders, K. M., Child, D. P., and Hotchkis, M. A. C.: A record of fallout 239Pu and 240Pu at World heritage bathurst harbour, Tasmania, Australia, J. Environ. Radioact., 237, 106679, https://doi.org/10.1016/j.jenvrad.2021.106679, 2021.

Haynes, D., Skinner, R., Tibby, J., Cann, J., and Fluin, J.: Diatom and foraminifera relationships to water quality in The Coorong, South Australia, and the development of a diatom-based salinity transfer function, J. Paleolimnol., 46, 543–560, https://doi.org/10.1007/s10933-011-9508-y, 2011.

https://doi.org/10.5194/egusphere-2026-6649
Preprint. Discussion started: 13 November 2026
© Author(s) 2026. CC BY 4.0 License.



991 Higgins, P. A., Palmer, J. G., Andersen, M. S., Turney, C. S. M., Johnson, F., Allen, K., Verdon-Kidd,
992 D., and Cook, E. R.: Examining past and projecting future: an 800-year streamflow reconstruction of
993 the Australian Murray river, Environ. Res. Lett., 18, 104016, https://doi.org/10.1088/1748-
994 9326/acf8d9, 2023.

995 Hogg, A. G., Heaton, T. J., Hua, Q., Palmer, J. G., Turney, C. S. M., Southon, J., Bayliss, A., Blackwell,
996 P. G., Boswijk, G., and Ramsey, C. B.: SHCal20 Southern Hemisphere calibration, 0–55,000 years cal
997 BP, Radiocarbon, 62, 759–778, https://doi.org/10.1017/RDC.2020.59, 2020.

998 Holgate, C. M., Van Dijk, A., Evans, J. P., and Pitman, A. J.: Local and remote drivers of southeast
999 Australian drought, Geophys. Res. Lett., 47, e2020GL090238, https://doi.org/10.1029/2020GL090238,
1000 2020.

1001 Holgate, C. M., Falster, G. M., Gillett, Z. E., Goswami, P., Grant, M. O., Hobeichi, S., Hoffmann, D.,
1002 Jiang, X., Jin, C., and Lu, X.: Physical mechanisms of meteorological drought development,
1003 intensification and termination: an Australian review. Communications Earth & Environment, 6 (1),
1004 220, https://doi.org/10.1038/s43247-025-02179-3, 2025.

1005 Holmes, J., Burn, M., Cisneros-Dozal, L. M., Jones, M., and Metcalfe, S.: An 1800-year oxygen-isotope
1006 record of short-and long-term hydroclimate variability in the northern neotropics from a Jamaican marl
1007 lake, Quat. Sci. Rev., 301, 107930, https://doi.org/10.1016/j.quascirev.2022.107930, 2023.

1008 Hotchkis, M. A. C., Child, D. P., Froehlich, M. B., Wallner, A., Wilcken, K., and Williams, M.:
1009 Actinides AMS on the VEGA accelerator, Nucl. Instruments Methods Phys. Res. Sect. B Beam Interact.
1010 with Mater. Atoms, 438, 70–76, https://doi.org/10.1016/j.nimb.2018.07.029, 2019.

1011 Huybers, K., Rupper, S., and Roe, G. H.: Response of closed basin lakes to interannual climate
1012 variability, Clim. Dyn., 46, 3709–3723, https://doi.org/10.1007/s00382-015-2798-4, 2016.

1013 Jeffrey, S. J., Carter, J. O., Moodie, K. B., and Beswick, A. R.: Using spatial interpolation to construct
1014 a comprehensive archive of Australian climate data, Environ. Model. Softw., 16, 309–330,
1015 https://doi.org/10.1016/S1364-8152(01)00008-1, 2001.

1016 John, J.: The Diatom Flora of Australia: Diatoms from Stradbroke and Fraser Islands, Queensland,
1017 Koeltz Botanical Books, Oberreifenberg, https://koeltz.com/en/johnjacob-diatom-flora-of-australia-
1018 volume-1-2016, 2016.

1019 John, J.: The Diatom Flora of Australia: Diatoms from Tasmania, Koeltz Botanical Books,
1020 Oberreifenberg, https://koeltz.com/en/johnjacob-diatom-flora-of-australia-volume-22018, 2018.

1021 John, J.: The Diatom Flora of Australia: Diatoms from Arid Australia, Koeltz Botanical Books,
1022 Oberreifenberg, https://koeltz.com/en/diatom-flora-of-australia-vol-3-diatoms-of-arid-australia-

https://doi.org/10.5194/egusphere-2026-6649
Preprint. Discussion started: 13 November 2026
© Author(s) 2026. CC BY 4.0 License.

taxonomy-and-biogeography-2019-4to-hardcoverisbn-978-3-946583-25-7, 2020.

Jones, R. N., McMahon, T. A., and Bowler, J. M.: Modelling historical lake levels and recent climate change at three closed lakes, Western Victoria, Australia (c. 1840–1990), J. Hydrol., 246, 159–180, https://doi.org/10.1016/S0022-1694(01)00369-9, 2001.

Juggins, S.: Quantitative reconstructions in palaeolimnology: new paradigm or sick science?, Quat. Sci. Rev., 64, 20–32, https://doi.org/10.1016/j.quascirev.2012.12.014, 2013.

Juggins, S.: C2: Software for ecological and palaeoecological data analysis and visualisation, User guide Version 1.8, https://www.staff.ncl.ac.uk/stephen.juggins/software/C2Home.htm, 2022.

Juggins, S.: rioja: Analysis of Quaternary Science Data, R package version 1.0-7, CRAN, https://doi.org/10.32614/CRAN.package.rioja, 2024.

Kemp, J., Radke, L. C., Olley, J., Juggins, S., and De Deckker, P.: Holocene lake salinity changes in the Wimmera, southeastern Australia, provide evidence for millennial-scale climate variability, Quat. Res., 77, 65–76, https://doi.org/10.1016/j.yqres.2011.09.013, 2012.

Kerfriden, B., Boivin, S., Malou, O., Fendane, Y., Boukcim, H., Almalki, S. D., Rees, S. K., Lee, B. P.-H., Mohamed, A., and Aldabaa, A.: Rapid assessment of soil traits in hyperarid areas via XRF and locally weighted PLSR, Front. Soil Sci., 5, 1668732, https://doi.org/10.3389/fsoil.2025.1668732, 2025.

Kiem, A. S., Johnson, F., Westra, S., Van Dijk, A., Evans, J. P., O'donnell, A., Rouillard, A., Barr, C., Tyler, J., Thyer, M., Jakob, D., Woldemeskel, F., Bellie Sivakumar, &, and Mehrotra, R.: Natural hazards in Australia: droughts, Clim. Change, 139, 37–54, https://doi.org/10.1007/s10584-016-1798-7, 2016.

Kirono, D. G. C., Jones, R. N., and Kent, D. M.: Modelling future lake levels and salinity at three lakes, Western Victoria, Natl. Res. Flagships, Clim. Adapt. CSIRO–A Rep. Prep. Environ. Prot. Auth. Victoria, 2009.

Kociolek, J. P. and Herbst, D. B.: Taxonomy and distribution of benthic diatoms from Mono Lake, California, USA, Trans. Am. Microsc. Soc., 338–355, https://doi.org/10.2307/3226708, 1992.

Krammer, K. and Lange-Bertalot, H.: Süßwasserflora von Mitteleuropa. Bacillariophyceae 1: Bacillariaceae, Epithemiacaeae, Surrirellaceae, Fischer, Germany, 1986.

Krammer, K. and Lange-Bertalot, H.: Bacillariophyceae. 2. Teil: Bacillariaceae, Epithemiaceae, Surirellaceae, Gustav Fischer Verlag, Stuttgart, 1988.

Krammer, K. and Lange-Bertalot, H.: Süßwasserflora von Mitteleuropa. Bacillariophyceae 3: Centrales, Fragilariaceae, Eunotiaceae, Fischer, Germany, 1991a.

https://doi.org/10.5194/egusphere-2026-6649
Preprint. Discussion started: 13 November 2026
© Author(s) 2026. CC BY 4.0 License.

Krammer, K. and Lange-Bertalot, H.: Süßwasserflora von Mitteleuropa. Bacillariophyceae 4: Acnanthaceae, Fischer, Germany, 1991b.

Laird, K. R., Kingsbury, M. V, Lewis, C. F. M., and Cumming, B. F.: Diatom-inferred depth models in 8 Canadian boreal lakes: inferred changes in the benthic: planktonic depth boundary and implications for assessment of past droughts, Quat. Sci. Rev., 30, 1201–1217, https://doi.org/10.1016/j.quascirev.2011.02.009, 2011.

Lavery, P. B. and Mead, D. J.: Pinus radiata: a narrow endemic from North America takes on the world. In: Richardson DM (ed) Ecology and Biogeography of Pinus, Cambridge Univ. Press., 432–449, 1998.

Leahy, P.: Lakes in the western district of Victoria and climate change, EPA Publ., 1359, 61, https://www.researchgate.net/publication/265989107_Lakes_in_the_Western_District_of_Victoria_and_climate_change, 2010.

Lengyel, E., Kovács, A. W., Padisák, J., and Stenger-Kovács, C.: Photosynthetic characteristics of the benthic diatom species Nitzschia frustulum (Kützing) Grunow isolated from a soda pan along temperature-, sulfate- and chloride gradients, Aquat. Ecol., 49, 401–416, https://doi.org/10.1007/s10452-015-9533-4, 2015.

Liu, M., Prentice, I. C., Ter Braak, C. J. F., and Harrison, S. P.: An improved statistical approach for reconstructing past climates from biotic assemblages, Proceedings. Math. Phys. Eng. Sci., 476, 20200346, https://doi.org/10.1098/rspa.2020.0346, 2020.

Ljungqvist, F. C., Piermattei, A., Seim, A., Krusic, P. J., Büntgen, U., He, M., Kirdyanov, A. V, Luterbacher, J., Schneider, L., and Seftigen, K.: Ranking of tree-ring based hydroclimate reconstructions of the past millennium, Quat. Sci. Rev., 230, 106074, https://doi.org/10.1016/j.quascirev.2019.106074, 2020.

McGowan, H. A., Marx, S. K., Denholm, J., Soderholm, J., and Kamber, B. S.: Reconstructing annual inflows to the headwater catchments of the Murray River, Australia, using the Pacific Decadal Oscillation, Geophys. Res. Lett., 36, https://doi.org/10.1029/2008GL037049, 2009.

McKay, R. C., Boschat, G., Rudeva, I., Pepler, A., Purich, A., Dowdy, A., Hope, P., Gillett, Z. E., and Rauniyar, S.: Can southern Australian rainfall decline be explained? A review of possible drivers, Wiley Interdiscip. Rev. Clim. Chang., 14, e820, https://doi.org/10.1002/wcc.820, 2023.

Mertens, A., van der Wal, J., Verweij, G., Pex, B., van Dulmen, A., and van Dam, H.: A revised list of diatom ecological indicator values in The Netherlands, Ecol. Indic., 172, 113219, https://doi.org/10.1016/j.ecolind.2025.113219, 2025.

Mills, K., Gell, P. A., and Kershaw, A. P.: The Recent Victorian Drought and its Impact: Without

https://doi.org/10.5194/egusphere-2026-6649
Preprint. Discussion started: 13 November 2026
© Author(s) 2026. CC BY 4.0 License.

Precedent?, Rural Industries Research and Development Corporation, https://www.academia.edu/78469514/The_Recent_Victorian_Drought_and_its_Impact_Without_Precedent, 2013.

Mondal, M. N., Horikawa, K., Seki, O., Nejigaki, K., Minami, H., Murayama, M., and Okazaki, Y.: Investigation of adequate calibration methods for X-ray fluorescence core scanning element count data: A case study of a marine sediment piston core from the Gulf of Alaska, J. Mar. Sci. Eng., 9, 540, https://doi.org/10.3390/jmse9050540, 2021.

Neukom, R., Steiger, N., Gómez-Navarro, J. J., Wang, J., and Werner, J. P.: No evidence for globally coherent warm and cold periods over the preindustrial Common Era, Nature, 571, 550–554, https://doi.org/10.1038/s41586-019-1401-2, 2019.

O'Donnell, A. J., McCaw, W. L., Cook, E. R., and Grierson, P. F.: Megadroughts and pluvials in southwest Australia: 1350–2017 CE, Clim. Dyn., 57, 1817–1831, https://doi.org/10.1007/s00382-021-05782-0, 2021.

Oksanen, J., Simpson, G. L., Blanchet, F. G., Kindt, R., Legendre, P., Minchin, P. R., O'Hara, R. B., Solymos, P., Stevens, M. H. H., Szoecs, E., and Wagner, H.: vegan: Community Ecology Package (version 2.7-2), https://doi.org/10.32614/CRAN.package.vegan, 2025.

Van Ommen, T. D. and Morgan, V.: Snowfall increase in coastal East Antarctica linked with southwest Western Australian drought, Nat. Geosci., 3, 267–272, https://doi.org/10.1038/ngeo761, 2010.

Palmer, J. G., Verdon-Kidd, D., Allen, K. J., Higgins, P., Cook, B. I., Cook, E. R., Turney, C. S. M., and Baker, P. J.: Drought and deluge: the recurrence of hydroclimate extremes during the past 600 years in eastern Australia's Natural Resource Management (NRM) clusters, Nat. Hazards, 120, 3565–3587, https://doi.org/10.1007/s11069-023-06288-0, 2024.

Rahman, M., Duxbury, L., Cadd, H., Klaebe, R., Jacobsen, G., Tibby, J., and Tyler, J.: A 2000-year record of hydroclimate variability inferred from oxygen isotopes in lake sediments on Kangaroo Island (Karti/Karta), South Australia, Quat. Sci. Rev., 363, 109443, https://doi.org/10.1016/j.quascirev.2025.109443, 2025.

Rahman, M., Tyler, J., Barr, C., Reid, M., Gell, P., and Tibby, J.: Development of a diatom-electrical conductivity transfer function for temperate Australian lakes, Manuscript submitted to Hydrobiologia (HYDR-S-26-01541), 2026.

Reid, M. A., Tibby, J. C., Penny, D., and Gell, P. A.: The use of diatoms to assess past and present water quality, Aust. J. Ecol., 20, 57–64, https://doi.org/10.1111/j.1442-9993.1995.tb00522.x, 1995.

Renberg, I.: A procedure for preparing large sets of diatom slides from sediment cores, J. Paleolimnol.,

https://doi.org/10.5194/egusphere-2026-6649
Preprint. Discussion started: 13 November 2026
© Author(s) 2026. CC BY 4.0 License.

4, 87–90, https://doi.org/10.1007/BF00208301, 1990.

Risbey, J. S., Pook, M. J., McIntosh, P. C., Wheeler, M. C., and Hendon, H. H.: On the remote drivers of rainfall variability in Australia, Mon. Weather Rev., 137, 3233–3253, https://doi.org/10.1175/2009MWR2861.1, 2009.

Roberts, J., Plummer, C., Vance, T., van Ommen, T., Moy, A., Poynter, S., Treverrow, A., Curran, M., and George, S.: A 2000-year annual record of snow accumulation rates for Law Dome, East Antarctica, Clim. Past, 11, 697–707, https://doi.org/10.5194/cp-11-697-2015, 2015.

Saunders, K. M., Kamenik, C., Hodgson, D. A., Hunziker, S., Siffert, L., Fischer, D., Fujak, M., Gibson, J. A. E., and Grosjean, M.: Late Holocene changes in precipitation in northwest Tasmania and their potential links to shifts in the Southern Hemisphere westerly winds, Glob. Planet. Change, 92, 82–91, https://doi.org/10.1016/j.gloplacha.2012.04.005, 2012.

Schofield, M. R., Barker, R. J., Gelman, A., Cook, E. R., and Briffa, K. R.: A model-based approach to climate reconstruction using tree-ring data, J. Am. Stat. Assoc., 111, 93–106, https://doi.org/10.1080/01621459.2015.1110524, 2016.

Sepúlveda-Zúñiga, E., Maidana, N. I., Villacís, L. A., Sagredo, E. A., and Moreno, P. I.: The last millennium viewed from a fine-resolution freshwater diatom record from northwestern Patagonia, Quat. Sci. Rev., 296, 107806, https://doi.org/10.1016/j.quascirev.2022.107806, 2022.

Smol, J. P. and Douglas, M. S. V: Crossing the final ecological threshold in high Arctic ponds, Proc. Natl. Acad. Sci., 104, 12395–12397, https://doi.org/10.1073/pnas.0702777104, 2007.

Spaulding, S. A. and al., et: Diatoms.org: supporting taxonomists, connecting communities, Diatom Res., 36, 291–304, https://doi.org/10.1080/0269249X.2021.2006790, 2021.

Steiger, N. J., Smerdon, J. E., Cook, E. R., and Cook, B. I.: A reconstruction of global hydroclimate and dynamical variables over the Common Era, Sci. Data, 5, 180086, https://doi.org/10.1038/sdata.2018.86, 2018.

Steinman, B. A., Abbott, M. B., Nelson, D. B., Stansell, N. D., Finney, B. P., Bain, D. J., and Rosenmeier, M. F.: Isotopic and hydrologic responses of small, closed lakes to climate variability: Comparison of measured and modeled lake level and sediment core oxygen isotope records, Geochim. Cosmochim. Acta, 105, 455–471, https://doi.org/10.1016/j.gca.2012.11.026, 2013.

Von Storch, H., Zorita, E., Jones, J. M., Dimitriev, Y., González-Rouco, F., and Tett, S. F. B.: Reconstructing past climate from noisy data, Science., 306, 679–682, https://doi.org/10.1126/science.1096109, 2004.

Taukulis, F. E. and John, J.: Development of a diatom-based transfer function for lakes and streams

https://doi.org/10.5194/egusphere-2026-6649
Preprint. Discussion started: 13 November 2026
© Author(s) 2026. CC BY 4.0 License.

severely impacted by secondary salinity in the south-west region of Western Australia, Hydrobiologia, 626, 129–143, https://doi.org/10.1007/s10750-009-9741-9, 2009.

Thöle, H., Bornemann, A., Heimhofer, U., Luppold, F. W., Blumenberg, M., Dohrmann, R., and Erbacher, J.: Using high-resolution XRF analyses as a sequence stratigraphic tool in a mudstone-dominated succession (Early Cretaceous, Lower Saxony Basin, Northern Germany), Depos. Rec., 6, 236–258, https://doi.org/10.1002/dep2.83, 2020.

Tibby, J. and Tiller, D.: Climate–water quality relationships in three Western Victorian (Australia) lakes 1984–2000, Hydrobiologia, 591, 219–234, https://doi.org/10.1007/s10750-007-0804-5, 2007.

Tibby, J., Reid, M. A., Fluin, J., Hart, B. T., and Kershaw, A. P.: Assessing long-term pH change in an Australian river catchment using monitoring and palaeolimnological data, Environ. Sci. Technol., 37, 3250–3255, https://doi.org/10.1021/es0263644, 2003.

Tibby, J., Gell, P. A., Fluin, J., and Sluiter, I. R. K.: Diatom–salinity relationships in wetlands: assessing the influence of salinity variability on the development of inference models, Hydrobiologia, 591, 207–218, https://doi.org/10.1007/s10750-007-0803-6, 2007.

Tibby, J., Tyler, J. J., and Barr, C.: Post little ice age drying of eastern Australia conflates understanding of early settlement impacts, Quat. Sci. Rev., 202, 45–52, https://doi.org/10.1016/j.quascirev.2018.10.033, 2018.

Tozer, C. R., Vance, T. R., Roberts, J. L., Kiem, A. S., Curran, M. A. J., and Moy, A. D.: An ice core derived 1013-year catchment-scale annual rainfall reconstruction in subtropical eastern Australia, Hydrol. Earth Syst. Sci., 20, 1703–1717, https://doi.org/10.5194/hess-20-1703-2016, 2016.

Trobajo, R., Rovira, L., Mann, D. G., and Cox, E. J.: Effects of salinity on growth and on valve morphology of five estuarine diatoms, Phycol. Res., 59, 83–90, https://doi.org/10.1111/j.1440-1835.2010.00603.x, 2011.

Tyler, J. J., Mills, K., Barr, C., Sniderman, J. M. K., Gell, P. A., and Karoly, D. J.: Identifying coherent patterns of environmental change between multiple, multivariate records: an application to four 1000-year diatom records from Victoria, Australia, Quat. Sci. Rev., 119, 94–105, https://doi.org/10.1016/j.quascirev.2015.04.010, 2015.

Tylmann, W., Bonk, A., Goslar, T., Wulf, S., and Grosjean, M.: Calibrating 210Pb dating results with varve chronology and independent chronostratigraphic markers: problems and implications, Quat. Geochronol., 32, 1–10, https://doi.org/10.1016/j.quageo.2015.11.004, 2016.

Vance, T. R., van Ommen, T. D., Curran, M. A. J., Plummer, C. T., and Moy, A. D.: A millennial proxy record of ENSO and eastern Australian rainfall from the Law Dome ice core, East Antarctica, J. Clim.,

https://doi.org/10.5194/egusphere-2026-6649
Preprint. Discussion started: 13 November 2026
© Author(s) 2026. CC BY 4.0 License.

26, 710–725, https://doi.org/10.1175/JCLI-D-12-00003.1, 2013.

Vance, T. R., Roberts, J. L., Plummer, C. T., Kiem, A. S., and Van Ommen, T. D.: Interdecadal Pacific variability and eastern Australian megadroughts over the last millennium, Geophys. Res. Lett., 42, 129–137, https://doi.org/10.1002/2014GL062447, 2015.

Viana, J. C. C., Sifeddine, A., Turcq, B., Albuquerque, A. L. S., Moreira, L. S., Gomes, D. F., and Cordeiro, R. C.: A late Holocene paleoclimate reconstruction from Boqueirão Lake sediments, northeastern Brazil, Palaeogeogr. Palaeoclimatol. Palaeoecol., 415, 117–126, https://doi.org/10.1016/j.palaeo.2014.07.010, 2014.

Victoria's Forestry and Bushfire Heritage.: Frankston State Pine Plantation, https://victoriasforestsbushfireheritage.com/2022/01/17/frankston-state-pine-plantation/, 2022

Walling, D. E. and Meyers, R. A.: Fallout radionuclides and the study of erosion and sedimentation, Encycl. Sustain. Sci. Technol. Springer, 3705–3768, https://doi.org/10.1007/978-1-4419-0851-3_288, 2012.

Wang, L., Rioual, P., Panizzo, V. N., Lu, H., Gu, Z., Chu, G., Yang, D., Han, J., Liu, J., and Mackay, A. W.: A 1000-yr record of environmental change in NE China indicated by diatom assemblages from maar lake Erlongwan, Quat. Res., 78, 24–34, https://doi.org/10.1016/j.yqres.2012.03.006, 2012.

Weltje, G. J. and Tjallingii, R.: Calibration of XRF core scanners for quantitative geochemical logging of sediment cores: Theory and application, Earth Planet. Sci. Lett., 274, 423–438, https://doi.org/10.1016/j.epsl.2008.07.054, 2008.

Wilkins, D., Gouramanis, C., De Deckker, P., Fifield, L. K., and Olley, J.: Holocene lake-level fluctuations in Lakes Keilambete and Gnotuk, southwestern Victoria, Australia, The Holocene, 23, 784–795, https://doi.org/10.1177/0959683612471983, 2013.

Yang, X., Kamenik, C., Schmidt, R., and Wang, S.: Diatom-based conductivity and water-level inference models from eastern Tibetan (Qinghai-Xizang) Plateau lakes, J. Paleolimnol., 30, 1–19, https://doi.org/10.1023/A:1024703012475, 2003.

Zheng, X., Hope, G., and Mooney, S. D.: The reconstruction of water table depth over the past 3100 years in south-eastern Australia using testate amoebae and potential implications for Pacific climatic variability, Palaeogeogr. Palaeoclimatol. Palaeoecol., 679, 113264, https://doi.org/10.1016/j.palaeo.2025.113264, 2025.

Zolitschka, B., Brauer, A., Negendank, J. F. W., Stockhausen, H., and Lang, A.: Annually dated late Weichselian continental paleoclimate record from the Eifel, Germany, Geology, 28, 783–786, https://doi.org/10.1130/0091-7613(2000)28%3C783:ADLWCP%3E2.0.CO;2, 2000.

https://doi.org/10.5194/egusphere-2026-6649
Preprint. Discussion started: 13 November 2026
© Author(s) 2026. CC BY 4.0 License.



1214 Zou, Y., Wang, L., He, H., Liu, G., Zhang, J., Yan, Y., Gu, Z., and Zheng, H.: Application of a diatom
1215 transfer function to quantitative paleoclimatic reconstruction—a case study of Yunlong Lake,
1216 Southwest China, Front. Earth Sci., 9, 700194, https://doi.org/10.3389/feart.2021.700194, 2021.

1217